STUDY OF INDUCTION MOTOR DRIVE WITH DIRECT TORQUE CONTROL SCHEME AND INDIRECT FIELD ORIENTED CONTROL SCHEME USING SPACE VECTOR MODULATION

A THESIS SUBMITTED IN PARTIAL FULFILLMENT OF THE REQUIREMENTS FOR THE DEGREE OF

Master of Technology

In

Electrical Engineering

(Power Control and Drives)

By

Nirupama Patra

Roll No.-211EE2136

DEPARTMENT OF ELECTRICAL ENGINEERING

NATIONAL INSTITUTE OF TECHNOLOGY

ROURKELA, ORISSA, INDIA

June 2013

STUDY OF INDUCTION MOTOR DRIVE WITH DIRECT TORQUE CONTROL SCHEME AND INDIRECT FIELD ORIENTED CONTROL SCHEME USING SPACE VECTOR MODULATION

A THESIS SUBMITTED IN PARTIAL FULFILLMENT OF THE REQUIREMENTS FOR THE DEGREE OF

Master of Technology

In

Electrical Engineering

(Power Control and Drives)

By

Nirupama Patra

Under the Guidance of

Prof. K.B.Mohanty

DEPARTMENT OF ELECTRICAL ENGINEERING

NATIONAL INSTITUTE OF TECHNOLOGY

ROURKELA-769008

NATIONAL INSTITUTE OF TECHNOLOGY

ROURKELA

CERTIFICATE

This is to certify that the work in this thesis entitled **"Study of Induction Motor Drive with Direct Torque Control scheme and Indirect field oriented control scheme using Space Vector Modulation "** submitted by **Nirupama Patra,** to the Department of Electrical Engineering, National Institute of Technology, Rourkela, in partial fulfillment of the requirements for the award of the degree of **Master of Technology** in "***Power Control and Drives***" is a bonafide work carried out by her under my supervision and guidance during the academic session 2012-2013.

Place:

Date:

Dr. K.B.Mohanty
Associate Professor
Dept. of Electrical Engineering
National Institute of Technology
Rourkela- 769008
India

ACKNOWLEDGEMENTS

On the submission of my thesis on **"Study of Induction Motor Drive with Direct Torque Control scheme and Indirect field oriented control scheme using Space Vector Modulation"**, I would like to articulate my deep gratitude and sincere thanks to my supervisor **Prof. Kanungo Barada Mohanty** for his most valuable guidance and thoughtful suggestions during the course of my work throughout the year. His help and advice has been a constant source of inspiration.

I am sincerely thankful to **Prof. A.K.Panda,** Head of the Department, Electrical Engg. and all the faculty members for providing a solid background for my studies and research thereafter. I am thankful to the laboratory staff of the department for their timely help.

An assemblage of this nature could never have been attempted without reference to and inspiration from the works of others whose details are mentioned in reference section. I acknowledge my indebtedness to all of them.

I am thankful to all my classmates and the department research scholars for their co-operation and unfailing help during the project work.

I am grateful to all my friends who made my stay in Rourkela, an unforgettable and rewarding experience.

Finally, I feel great reverence for all my family members and the Almighty, for their blessings and for being a constant source of encouragement.

Nirupama Patra

DEDICATED TO

MY BELOVED

PARENTS

ABSTRACT

Induction motors are the starting point to design an electrical drive system which is widely used in many industrial applications. In modern control theory, different mathematical models describe induction motor according to the employed control methods. Vector control strategy can be applied to this electrical motor type in symmetrical three phase version or in unsymmetrical two phase version. The operation of the induction motor can be analyzed similar to a DC motor through this control method. With the Joint progress of the power electronics and numerical electronics it is possible today to deal with the axis control with variable speed in low power applications. With these technological projections, various command approaches have been developed by the scientific community to master in real time, the flux and the torque of the electrical machines, the direct torque control (DTC) scheme being one of the most recent steps in this direction. This scheme provides excellent properties of regulation without rotational speed feedback. In this control scheme the electromagnetic torque and stator flux magnitude are estimated with only stator voltages and currents and this estimation does not depend on motor parameters except for the stator resistance.

In this dissertation report conventional DTC scheme has been described. Induction motor has been simulated in stationary d-q reference frame and its free acceleration characteristics are drawn. Conventional DTC scheme has been simulated with a 50 HP, 460V, 60Hz induction motor. Literature review has been done to study the recent improvements in DTC scheme which somehow is able to overcome the drawbacks of conventional one.

The space vector modulation technique (SVPWM) is applied to 2 level inverter control in the vector control based induction motor drive system, thereby dramatically reducing the torque ripple. Later in this project space vector PWM technique will be applied to DTC drive system to reduce the torque ripple.

CONTENTS

CHAPTERS

LIST OF SYMBOLS

Subscripts:

a, b, c : for A, B, C phase sequence components respectively

s, r : for stator and rotor quantities respectively

q, d : for quadrature and direct axis components

0 : for zero sequence components

l : for leakage quantities

em : for electromagnetic (e.g. T_{em} = electromagnetic torque)

sl : for slip quantities

b : for base quantities

m : for magnetizing component

Superscript

s, r : for quantities in stationary and rotor reference frame respectively

e : for synchronously rotating reference frame

, (dash) : for referring rotor quantities to stator side

* (star) : for the command values of quantities in simulation model

abc : for matrix notation of any phase quantities

qd0 : for matrix notation of any *q, d, 0* quantities

Symbols

IM	Induction motor
IMD	Induction motor drives
ASD	Adjustable speed drives
v	voltage in Volts
i	current in Amperes
z	impedance in Ohms
R	resistance in Ohms
t	time in sec
N	speed in rpm
Phi	flux in Wb
ψ	flux linkage in Volts.sec
L	inductance in Henry
x	reactance in ohms
ω	angular speed in rad/sec
θ	phase angle in rad
Δ	small change
ϕ	phase
T	torque in Nm
P	no of poles
p	differential operator
n	stator to rotor turn ratio

LIST OF FIGURES

LIST OF TABLES

CHAPTER-1

INTRODUCTION

1.1Induction motor drives

Over the past decades DC machines were used extensively for variable speed applications due to the decoupled control of torque and flux that can be achieved by armature and field current control respectively. DC drives are advantageous in many aspects as in delivering high starting torque, ease of control and nonlinear performance. But due to the major drawbacks of DC machine such as presence of mechanical commutator and brush assembly, DC machine drives have become obsolete today in industrial applications.

The robustness, low cost, the better performance and the ease of maintenance make the asynchronous motor advantageous in many industrial applications or general applications. Squirrel cage induction motors (SCIM) are more widely used than all the rest of the electric motors as they have all the advantages of AC motors and are cheaper in cost as compared to Slip Ring Induction motors; require less maintenance and rugged construction. Because of the absence of slip rings, brushes maintenance duration and cost associated with the wear and tear of brushes are minimized. Due to these advantages, the induction motors have been the execution element of most of the electrical drive system for all related aspects: starting, braking, speed change and speed reversal etc.

To reach the best efficiency of induction motor drive (IMD), many new techniques of control has been developed in the last few years. Now-a-days, using modern high switching frequency power converters controlled by microcontrollers, the frequency, phase and magnitude of the input to an AC motor can be changed, hence the motor speed and torque can be controlled. Today, it is possible to deal with the axis control of machine drives with variable speed in low power applications mostly due to joint progress of the power electronics and numerical electronics. The dynamic operation of the induction machine drive system has an important role on the overall performance of the system of which it is a part.

In **1986 Takahashi and Noguchi** [3] proposed a new technique for the control of induction motor, quite different from field oriented control based on limit cycle control of both torque and flux using optimum PWM output voltage which gives quick torque response and is highly efficient. Here efficiency optimisation in steady state operation has been considered and

this proposed control circuit has the disadvantage of making some drift in extremely low frequency operation which can however be compensated easily and automatically to minimise the effect of variation of machine constant.

Thomas G Habetler [4] in **1992** proposed a direct torque control method of induction machine based on predictive, deadbeat control of the torque and flux. Here the change in torque and flux, over the switching period is calculated by estimating the synchronous speed and the voltage behind the transient reactance and the stator voltage is calculated which is required to cause the torque and flux to be equal to their respective reference values. Then Space vector PWM is used to define the inverter switching state. To be used in the transient or pulse dropping mode, an alternative approach to deadbeat control is also presented.

Vector control of induction motor without encoder was proposed by **James N Nash** [6] in **1997.** Here an explanation of direct self-control and the field orientation concept, implemented in adaptive motor model is presented and also the reliance of the control method on fast processing techniques has been stressed.

A new scheme of direct torque control of induction motor for electric vehicles[10]was proposed in **2004 by M.vasudevan and Dr. R.Arumugan,** this electric vehicle drive consists of rewound induction motors and a three-level IGBT inverter. Field Oriented Control, Direct Torque Control (DTC), and DTC using Space Vector Modulation are investigated here and also a comparison between these control schemes is presented. DTC using Space vector modulation is found to be the best scheme for this application.

A detailed comparison between viable adaptive intelligent torque control strategies of induction motor [11] was presented by **M.Vasudevan, R.Arumugan and S.Paramasivam** in **2005** emphasizing its advantages and disadvantages. The performance of neural network, fuzzy and genetic algorithm based torque controllers is evaluated as the various sensorless DTC techniques of IM. These adaptive intelligent techniques are applied to achieve high performance decoupled flux and torque control.

In **2008 Sarat K Sahoo, Tulsiram Das, Vedam Subrahmanyam** [12] presented a simple approach to design and implementation of Direct Torque Control (DTC) of three phase squirrel cage induction motor using Matlab/Simulink and FPGA software[18]. Two simple new techniques i.e. constant switching frequency and stator flux estimation are proposed to maintain this simple control structure of DTC while at the same time improving the performance of the

DTC drives. A simple torque control is introduced to replace the three level hysteresis comparators to maintain a constant switching frequency. By using simple compensator based on steady state operation, the magnitude and phase error associated with stator flux estimation based on voltage model is compensated.

A strategy of variable duty ratio control scheme is proposed by **Prof.K.B.Mohanty in 2009**[15] to increase switching frequency, and adjust the width of hysteresis bands of conventional DTC according to the switching frequency. This technique minimizes torque and current ripples, improves torque response, and reduces switching losses in spite of its simplicity.

Direct torque control of induction motor using space vector pulse width modulation technique was described by **S.L.Kaila and H.B.Jani** in **2011**. The switching instants of different space vectors are determined for each sampling period in order to minimize the torque ripple in SVPWM technique.

1.2 Types of control schemes

There are two important steps to design a control system for electrical drives

1. In order to accomplish the analysis and the evaluation of the system, first the drive system has to be converted into a mathematical model.
2. When external perturbations are present, through an optimal regulator the imposed response on the system is obtained.

There are two fundamental directions of IM control [1]

- **Analogue:** direct measurement of the machine parameters (mainly the rotor speed), which are compared to the reference signals through closed control loops.
- **Digital:** estimation of the machine parameters in the sensorless control schemes (without measuring the rotor speed).

The parameter estimation can be done by implementing following methodologies [1]

- Slip frequency calculation method
- Speed estimation using state equation;
- Estimation based on slot space harmonic voltages;
- Flux estimation and flux vector control;

•Direct control of torque and flux;

•Observer-based speed sensorless control;

•Model reference adaptive systems;

•Kalman filtering techniques;

•Sensorless control with parameter adaptation;

•Neural network based sensorless control;

•Fuzzy-logic based sensorless control.

Classification of control techniques for IM from the view point of the controlled signal [1] [2]:

- **Scalar control:** based on relationships valid in steady state, only magnitude and frequency of voltage, current and flux linkage space vectors are controlled. Disregards the coupling effect in the machine.
- **Vector control:** based on relations valid in dynamics state, not only magnitude and frequency but also instantaneous position of voltage, current and flux linkage space vector are controlled. The most popular vector control methods are the Field oriented control (FOC) and DTC.

Scalar controlled drives give somewhat inferior performance, but easy to implement. Their importance has been diminished recently because of the superior performance of vector controlled drives which is demanded in many applications [5].

1.2 Direct torque control

DTC was first introduced by Takahashi in 1984 in Japan and by Dopenbrock in 1985 in Germany [3] [7] and today this control scheme is considered as the world's most advanced AC Drives control technology. This is a simple control technique which does not require coordinate transformation, PI regulators, and Pulse width modulator and position encoders [20] [25].This technique results in direct and independent control of motor torque and flux by selecting optimum inverter switching modes. The electromagnetic torque and stator flux are calculated from the primary motor inputs e.g. stator voltages and currents [16]. The optimum voltage vector selection for the inverter is made so as to restrict the torque and flux errors within the hysteresis bands. The

advantages of this control technique are quick torque response in transient operation and improvement in the steady state efficiency.

1.4 MOTIVATION

The electric drives used in industry are Adjustable Speed Drives and in most of these drives AC motors are applied. Induction motors are the standard in these drives. Induction motors are today the most widely used ac machines due to the advantageous mix of low cost, reliability and performance. So effective control of IM parameters e.g. speed, torque and flux is of utmost importance. From the investigation of the control methods it is known that torque control of IM can be achieved according to different techniques ranging from inexpensive Volts/Hz ratio strategy to sophisticated sensorless vector control scheme. But every method has its own disadvantages like losses, need of separate current control loop, coordinate transformation (thus increasing the complexity of the controller), torque and current ripple etc.So it is very much necessary to design a controller to obtain an ideal electric vehicle motor drive system which would have high efficiency, low torque ripple and minimum current distortion.

1.5 OBJECTIVE

The main objective of this project work is to develop; 1. a control method in order to achieve superior dynamic response, fast torque response 2.a controller having low inverter switching frequency, low harmonic losses, high efficiency. The DTC controller has all the above characteristics to be good a controller. So the objective here is to study the most advanced IM control method i.e. direct torque control and investigate its performance characteristics.

1.6 OVERVIEW OF THE THESIS

Chapter 2: discusses the mathematical model of three phase induction motor, the concept of reference frames and the induction motor dynamic equations in various reference frames, the equations in stationary reference frame are to be applied on further chapters. A brief description of voltage source inverter is also given in this chapter. A Simulink model of induction motor in stationary reference frame is given.

Chapter 3: introduces the conventional DTC scheme, discusses DTC principle and various methods of estimating stator flux in detail, a brief idea about the hysteresis controllers is given.

Chapter 4: discusses the basic concept of space vector modulation, pulse pattern generation and application of space vector pulse width modulation technique to indirect vector control strategy.

Chapter 5: Conventional DTC scheme is simulated by MATLAB/SIMULINK platform. The model is run for typical conditions of reference speed and applied torque values. Initially the starting transient of DTC drive for no load condition is observed and later performance of machine for speed reversal is checked. Flux plot of DTC drive is also shown. Characteristics of motor for indirect vector control based on SVPWM are shown finally.

Chapter 6: gives summery of the whole work, the conclusion and directions for future work.

CHAPTER 2

VOLTAGE SOURCE INVERTER FED INDUCTION MOTOR DRIVES

2.1 Introduction

The type of waveforms that the electric drive system deals with is ac waveforms, so the main objective of power converters needed in adjustable speed drives (ASDs) should produce an ac output waveform from a dc power supply. The magnitude, frequency, and phase of the sinusoidal ac outputs should be controllable. According to the type of ac output waveform, the power converter topologies can be considered as voltage source inverters (VSIs) and current source inverters (CSIs). The voltage source inverters, where the ac output voltage waveform can be controlled independently, is the most widely used power converters in ASDs and many industrial applications because they naturally behave as voltage sources as required in these applications. The output of the VSI is fed to the three phase induction motor which is finally connected to the load of the drive system.

2.2 Dynamic model of induction motor

The stator of induction motor consists of three phase balanced distributed windings with each phase separated from other two windings by 120 degrees in space [1]. When current flows through these windings, three phase rotating magnetic field is produced. The dynamic behavior of the induction machine is taken into account in an adjustable speed drive system using a power electronics converter. This machine constitutes an element within a feedback loop. Study of the dynamic performance of the machine is complex due to coupling effect of the stator and rotor windings, also the coupling coefficient varies with rotor position. So a set of differential equations with time varying coefficients describe the machine model [1].

To derive the dynamic model of the machine, the following assumptions are made:

- No magnetic saturation;
- No saliency effects i.e. machine inductance is independent of rotor position;
- Stator windings are so arranged as to produce sinusoidal mmf distributions;
- Effects of the stator slots may be neglected;
- No fringing of the magnetic circuit;

- Constant magnetic field intensity, radially directed across the air-gap;
- Negligible eddy current and hysteresis effects;

A balanced three phase supply is given to the motor from the power converter. For dynamic modeling of the motor two axes theory is used [1]. According to this theory the time varying parameters can be expressed in mutually perpendicular direct (*d*) and quadrature (*q*) axis. For the representation of the *d*-*q* dynamic model of the machine a stationary or rotating reference frame is assumed.

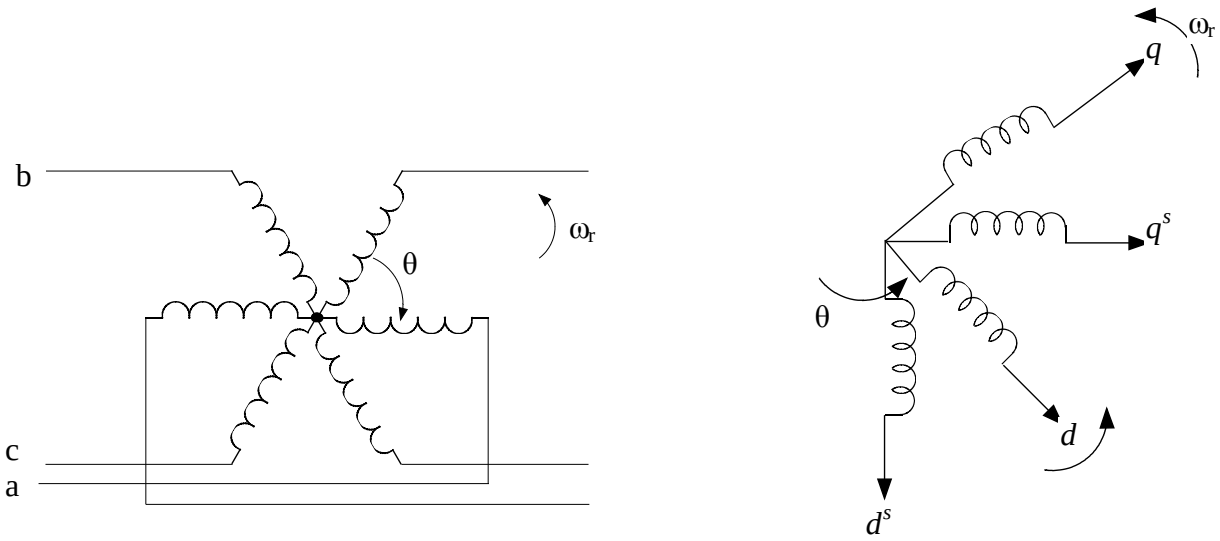

Fig.2.1 (a) Coupling effect in stator and rotor winding of motor (b) Equivalent two-phase machine

In stationary reference frame the d^s and q^s axes are fixed on the stator, whereas these are rotating at an angle with respect to the rotor in rotating reference frame. The rotating reference frame may either be fixed on the rotor or it may be rotating at synchronous speed. In synchronously rotating reference frame with sinusoidal supply the machine variables appear as dc quantities in steady state condition [24].

2.2.1 Axes transformation

(a) Three phase to two phase transformation

A symmetrical three phase machine is considered with stationary *as*-*bs*-*cs* axes at 120 degree apart as shown in fig.2.2.

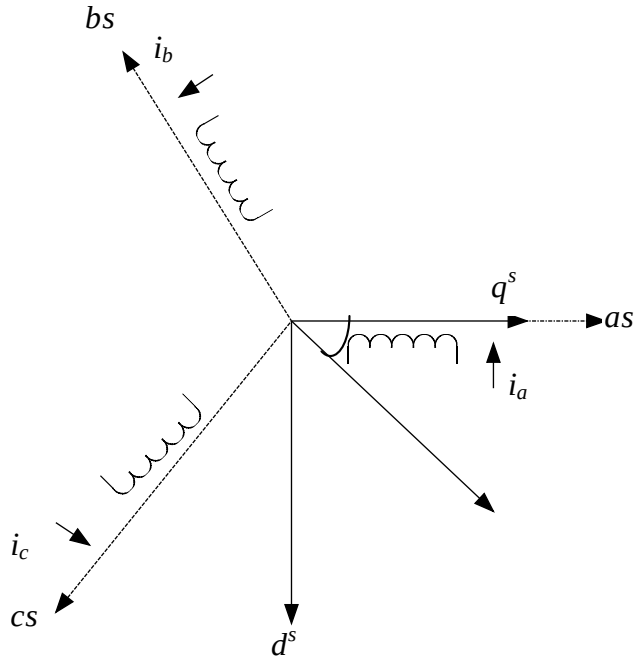

Fig.2.2 *as-bs-cs* to d^s-q^s axis transformation (θ = 0)

The voltages v_{as}, v_{bs}, v_{cs} are the voltages of *as*, *bs*, *cs* phases respectively. Now assuming that the stationary d^s-q^s axes are oriented at θ angle as shown and the voltages along d^s-q^s axes to be $v_{ds}{}^s$, $v_{qs}{}^s$ respectively, the stationary two phase voltages can be transformed to three phase voltages according to the following equations:

$$v_{as} = v_{qs}{}^s \cos\theta + v_{ds}{}^s \sin\theta \quad (2.1)$$

$$v_{bs} = v_{qs}{}^s \cos(\theta - 120°) + v_{ds}{}^s \sin(\theta - 120°) \quad (2.2)$$

$$v_{cs} = v_{qs}{}^s \cos(\theta + 120°) + v_{ds}{}^s \sin(\theta + 120°) \quad (2.3)$$

The phase voltages in matrix form can be written as:

$$\begin{bmatrix} v_{as} \\ v_{bs} \\ v_{cs} \end{bmatrix} = \begin{bmatrix} \cos\theta & \sin\theta & 1 \\ \cos(\theta - 120°) & \sin(\theta - 120°) & 1 \\ \cos(\theta + 120°) & \sin(\theta + 120°) & 1 \end{bmatrix} \begin{bmatrix} v_{qs}^s \\ v_{ds}^s \\ v_{0s}^s \end{bmatrix}$$

By inverse transformation, $v_{ds}{}^s$ and $v_{qs}{}^s$ can be written in terms of three phase voltages in matrix form as follows:

$$\begin{bmatrix} v_{qs}^{s} \\ v_{ds}^{s} \\ v_{0s}^{s} \end{bmatrix} = \frac{2}{3}\begin{bmatrix} \cos\theta & \cos(\theta-120°) & \cos(\theta+120°) \\ \sin\theta & \sin(\theta-120°) & \sin(\theta+120°) \\ 0.5 & 0.5 & 0.5 \end{bmatrix}\begin{bmatrix} v_{as} \\ v_{bs} \\ v_{cs} \end{bmatrix}$$

Where v_{0s} = zero sequence component which may or may not present.

For convenient q^s axis is aligned with the *as*-axis i.e. θ = 0 and zero sequence component is neglected. So the transformation relations are reduced to

$$v_{as} = v_{qs}^{s} \quad (2.4)$$

$$v_{bs} = -\frac{1}{2}v_{qs}^{s} - \frac{\sqrt{3}}{2}v_{ds}^{s} \quad (2.5)$$

$$v_{cs} = -\frac{1}{2}v_{qs}^{s} + \frac{\sqrt{3}}{2}v_{ds}^{s} \quad (2.6)$$

$$v_{qs}^{s} = v_{as} \quad (2.7)$$

$$v_{ds}^{s} = -\frac{1}{\sqrt{3}}(v_{bs} - v_{cs}) \quad (2.8)$$

(b) Two phase stationary to two phase synchronously rotating frame transformation

The stationary d^s-q^s axes are transformed to synchronously rotating d^e-q^e reference frame which is rotating at speed ω_e with respect to d^s-q^s axes with the help of fig.2.3.

The angle between d^s and d^e axes is $\theta_e = \omega_e t$. The voltages v_{ds}^{s}, v_{qs}^{s} can be converted to voltages on d^e-q^e axis according to the following relations:

$$v_{ds} = v_{qs}^{s}\cos\theta_e - v_{ds}^{s}\sin\theta_e \quad (2.9)$$

$$v_{qs} = v_{qs}^{s}\sin\theta_e + v_{ds}^{s}\cos\theta_e \quad (2.10)$$

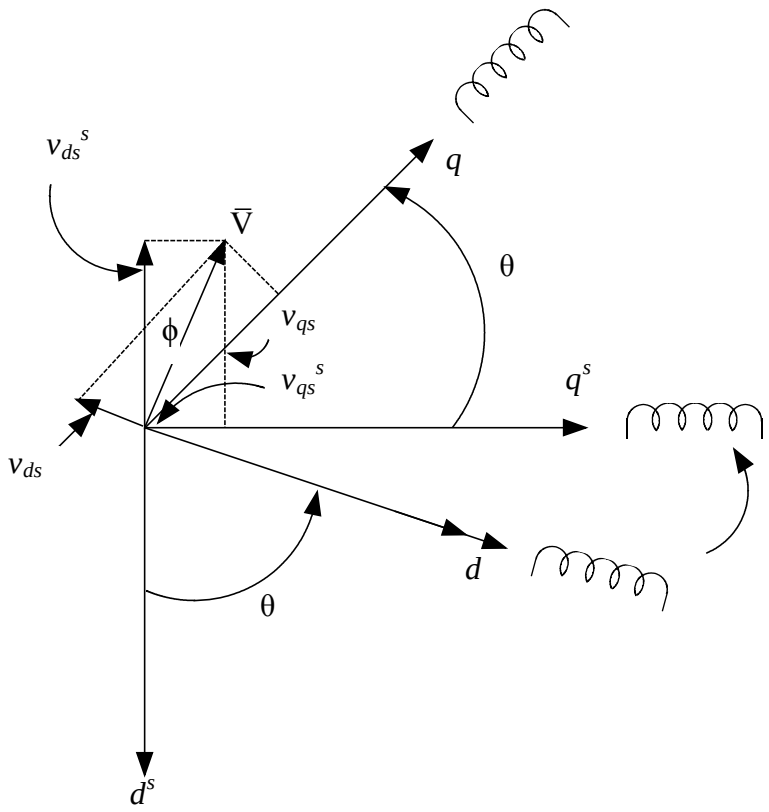

Fig.2.3 Stationary *d-q* frame to synchronously rotating frame transformation

The transformation of rotating frame parameters to stationary frame is according to the following relations:

$$v_{qs}^{s} = v_{qs}\cos\theta_e + v_{ds}\sin\theta_e \quad (2.11)$$

$$v_{ds}^{s} = -v_{qs}\sin\theta_e + v_{ds}\cos\theta_e \quad (2.12)$$

Assuming that the three phase voltages are balanced and sinusoidal given by following

$$v_{as} = V_m\cos(\omega_e t + \phi) \quad (2.13)$$

$$v_{bs} = V_m\cos(\omega_e t + \phi - 2\pi/3) \quad (2.14)$$

$$v_{cs} = V_m\cos(\omega_e t + \phi + 2\pi/3) \quad (2.15)$$

Substituting equations (2.13) – (2.15) in equations (2.8) and (2.9) we get

$$v_{qs}^{s} = V_m\cos(\omega_e t + \phi) \quad (2.16)$$

$$v_{ds}^{s} = -V_m\sin(\omega_e t + \phi) \quad (2.17)$$

Substituting (2.16) – (2.17) in (2.9) – (2.10)

$$v_{qs} = V_m \cos \phi \qquad (2.18)$$

$$v_{ds} = -V_m \sin(\phi) \qquad (2.19)$$

From equations (2.18) and (2.19) it is clear that sinusoidal quantities in a stationary frame appear as dc quantities in a synchronously rotating reference frame.

2.2.2 Motor dynamic model in stationary frame

Machine model in stationary frame by Stanley equations substituting $\omega_e = 0$. The stator circuit equations are written as:

$$v_{qs}^{\ s} = R_s i_{qs}^{\ s} + \frac{d}{dt}\psi_{qs}^{\ s} \qquad (2.20)$$

$$v_{ds}^{\ s} = R_s i_{ds}^{\ s} + \frac{d}{dt}\psi_{ds}^{\ s} \qquad (2.21)$$

$$0 = R_r i_{qr}^{\ s} + \frac{d}{dt}\psi_{qr}^{\ s} - \omega_r \psi_{dr}^{\ s} \qquad (2.22)$$

$$0 = R_r i_{dr}^{\ s} + \frac{d}{dt}\psi_{dr}^{\ s} + \omega_r \psi_{qr}^{\ s} \qquad (2.23)$$

Where $\psi_{qs}^{\ s}, \psi_{ds}^{\ s}$ = q-axis and d-axis stator flux linkages

$\psi_{qr}^{\ s}, \psi_{dr}^{\ s}$ = q-axis and d-axis rotor flux linkages

R_s , R_r = stator and rotor resistances

ω_r = rotor speed and $v_{dr} = v_{qr} = 0$

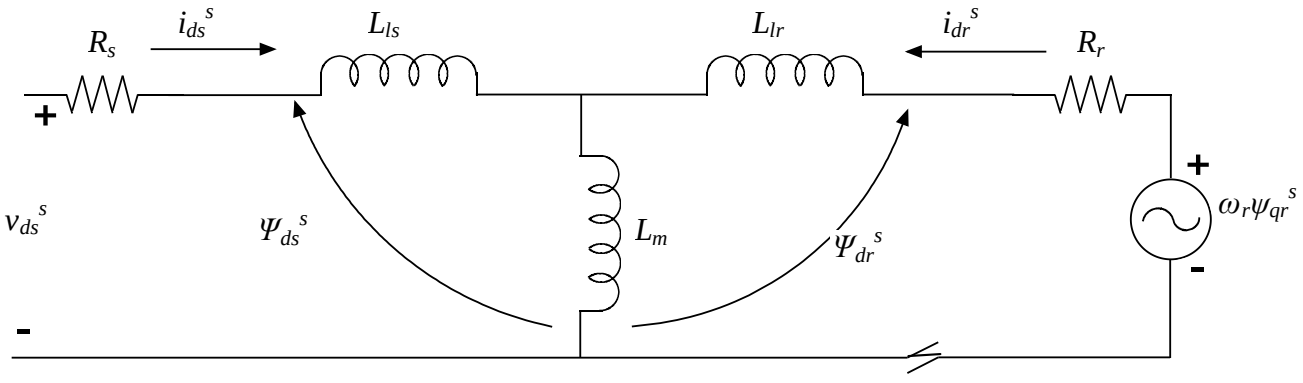

(a)

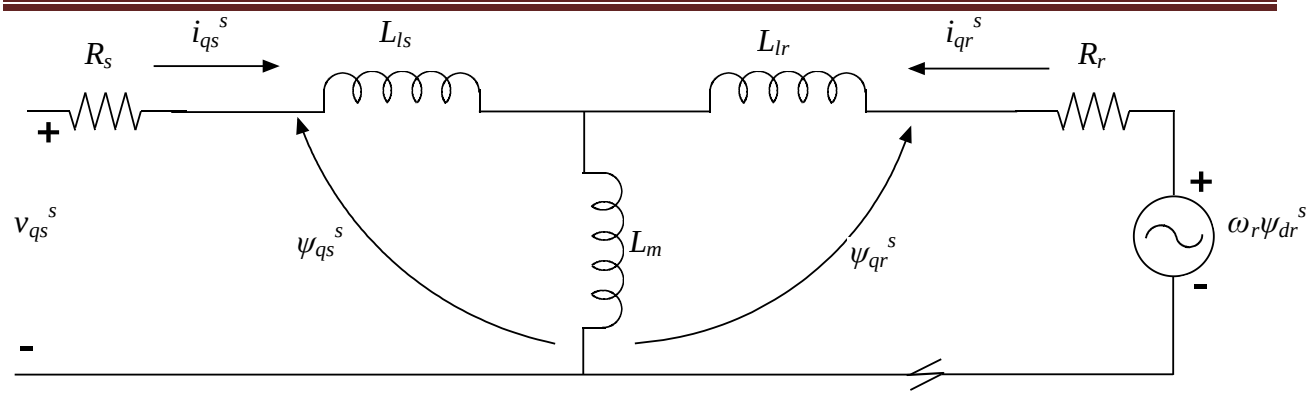

(b)

Fig.2.4 d^s-q^s equivalent circuits

The electromagnetic torque is developed by the interaction of air gap flux and rotor mmf which can be expressed in general vector form as

$$T_e = \frac{3}{2}\frac{P}{2}(\bar{\psi}_m) * (\bar{I}_r)$$

The torque equations can be written in stationary frame with corresponding variables as

$$T_e = \frac{3}{2}\frac{P}{2}(\psi_{dm}^{\ s} i_{qr}^{\ s} - \psi_{qm}^{\ s} i_{dr}^{\ s}) \quad (2.24)$$

$$= \frac{3}{2}\frac{P}{2}(\psi_{dm}^{\ s} i_{qs}^{\ s} - \psi_{qm}^{\ s} i_{ds}^{\ s}) \quad (2.25)$$

$$= \frac{3}{2}\frac{P}{2}(\psi_{ds}^{\ s} i_{qs}^{\ s} - \psi_{qs}^{\ s} i_{ds}^{\ s}) \quad (2.26)$$

$$= \frac{3}{2}\frac{P}{2}L_m(i_{dr}^{\ s} i_{qs}^{\ s} - i_{qr}^{\ s} i_{ds}^{\ s}) \quad (2.27)$$

$$= \frac{3}{2}\frac{P}{2}(\psi_{dr}^{\ s} i_{qr}^{\ s} - \psi_{qr}^{\ s} i_{dr}^{\ s}) \quad (2.28)$$

2.3 Voltage source inverter

In VSIs the input voltage is maintained constant and the amplitude of the output voltage is independent of the nature of the load. But the output current waveform as well as magnitude depends upon nature of load impedance. Three phase VSIs are more common for providing adjustable frequency power to industrial applications as compared to single phase inverters. The VSIs take dc supply from a battery or more usually from a 3-ϕ bridge rectifier.

A basic three phase VSI is a six step bridge inverter, consisting of minimum six power electronics switches (i.e. IGBTs, Thyristors) and six feedback diodes. A step can be defined as the change in firing from one switch to the next switch in proper sequence. For a six step inverter each step is of 60º interval for one cycle of 360º. That means the switches would be gated at regular intervals of 60º in proper sequence to get a three phase ac output voltage at the output terminal of VSI. Fig.2.5 shows the power circuit diagram of three phase VSI using six IGBTs and six diodes connected anti parallel to the IGBTs. The capacitor connected in to the input terminals is to maintain the input dc voltage constant and this also suppresses the harmonics fed back to the dc source. Three phase load is star connected.

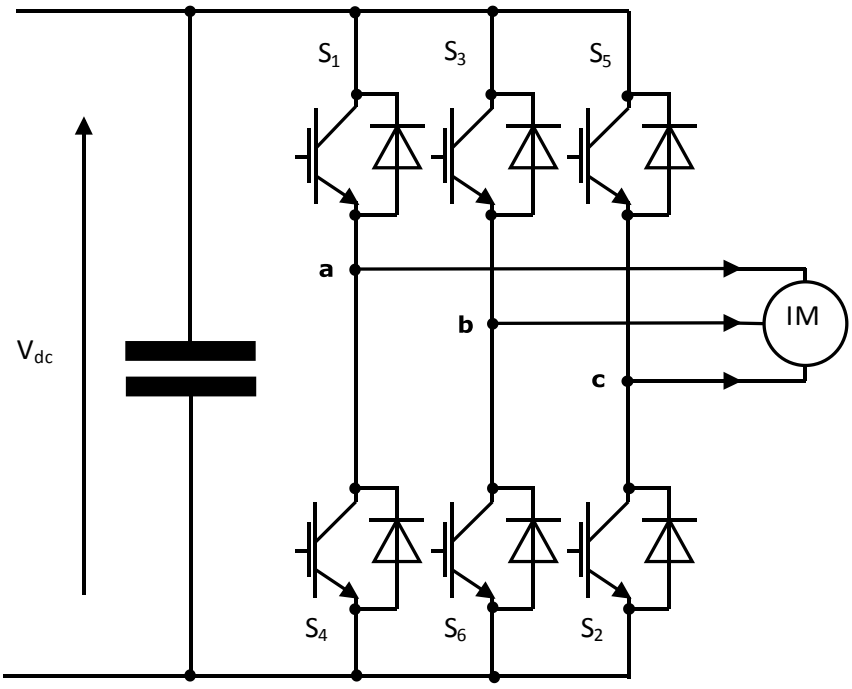

Fig.2.5 Three phase VSI using IGBTs

The six switches are divided into two groups; upper three switches as positive group (i.e. S_1, S_3, S_5) and lower three as negative group of switches (i.e. S_4, S_6, S_2). There are two possible gating patterns to the switches i.e. there are two conduction modes: 1. 180º conduction mode and 2. 120º conduction mode. In each pattern the gating signals are applied and removed at an interval of 60º of the output voltage waveform. In 180º mode three switches are on at a time, two from positive group and one from negative group or vice versa, each switch conducts for 180º of a cycle. In 120º mode each switch conduct for 120º in one cycle and two switches remain turned on at a time, one from positive group and one from negative group. But no two switches of the same leg should be turned on simultaneously in both cases as this condition would short circuit the dc source.

In 120º conduction mode the chances of short circuit of the dc link voltage source is avoided as each switch conduct for 120º in one cycle, so there is an interval of 60º in each cycle when no switch is in conduction mode and the output voltage at this time interval is zero. In general there is a 60º interval between turning off one switch and turning on of the complimentary switch in the same leg. This 60º interval is sufficient for the outgoing switch to regain its forward blocking capability.

The standard three-phase VSI topology has eight valid switching states which are given in Table.1. Of the eight valid switching states, two are zero voltage states(0 and 7 in Table.1) which produce zero ac line voltages and in this case, the ac line currents freewheel through either the upper or lower components. The remaining states (1 to 6 in Table.1) are active states which produce non-zero ac output voltages. The inverter moves from one state to another in order to generate a given voltage waveform. Thus the resulting ac output line voltages consist of discrete values of voltages such as $\frac{V_s}{2}, 0, -\frac{V_s}{2}$for the topology shown in Fig. 2.5. The corresponding output voltage waveform is shown in fig.2.6. In 180º mode of conduction the waveform of ac phase output voltage is stepped one having values $\frac{3V_s}{2}, \frac{V_s}{2}, 0, -\frac{V_s}{2}, -\frac{3V_s}{2}$and line voltage waveform is quasi-square wave type having discrete values$\frac{V_s}{2}, 0, -\frac{V_s}{2}$. In 120º mode the phase voltage waveform is quasi-square type.

Table 2.1 Switching states of a three phase VSI

State	S_a	S_b	S_c	Vector
0	0	0	0	V_0
1	1	0	0	V_1
2	1	1	0	V_2
3	0	1	0	V_3
4	0	1	1	V_4
5	0	0	1	V_5
6	1	0	1	V_6
7	1	1	1	V_7

2.4 Conclusion

In this chapter detail dynamic model of IM is discussed in stationary reference frame. In order to understand and design vector controlled drives the dynamic model of the machine to be controlled must be known which could be a good approximation of the real plant. To formulate the model two axis theory and space phasor notations have been used. It has been proved that space phasor notation is compact and easier to work with.

CHAPTER-3

DIRECT TORQUE CONTROL OF INDUCTION MOTOR

3.1 Introduction

In recent years "induction motor control techniques" have been the field of interest of many researchers to find out different solutions for induction motor control having the features of precise and quick torque response, and reduction of the complexity of field oriented control [3]-[7]. The Direct torque control (DTC) technique has been recognized as the simple and viable solution to achieve this requirements.DTC is one of the most excellent and efficient control strategies of induction motor. This technique is based on decoupled control of torque and stator flux and today it is one of the most actively researched control techniques where the aim is to control effectively the torque and flux.

3.1.1 Conventional DTC scheme

The conventional DTC scheme is a closed loop control scheme, the important elements of the control structure being: the power supply circuit, a three phase voltage source inverter, the induction motor, the speed controller to generate the torque command and the DTC controller. The DTC controller again consists of torque and flux estimation block, two hysteresis controllers and sector selection block, the output of the DTC controller is the gating pulses for the inverter.

The DTC scheme does not require coordinate transformation as all the control procedures are carried out in stationary frame of reference. So this scheme does not suffer from parameter variations to the extent that other control techniques do. Also there is no feedback current control loop due to which the control actions do not suffer from the delays inherent in the current controllers, no pulse width modulator, no PI controllers, and no rotor speed or position sensor. So it is a sensorless control technique which operates the motor without requiring a shaft mounted mechanical sensor. Here on-line torque and flux estimators are used for closing the loop. Here the torque and stator flux are controlled directly by using hysteresis comparators. Fig.3.1 shows the basic block diagram of conventional DTC scheme [8] [10].

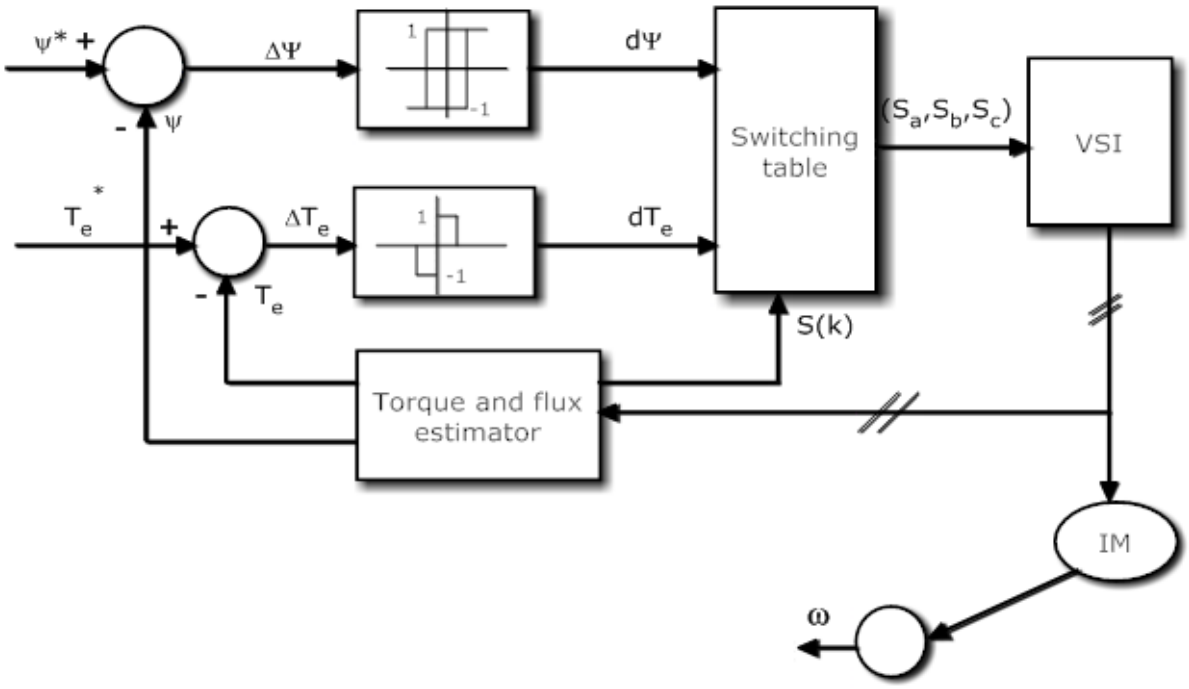

Fig.3.1 Block diagram of conventional DTC scheme for IM drives

3.2 Principle of DTC scheme

The basic principle of DTC is to directly select stator voltage vectors according to the torque and flux errors which are the differences between the references of torque and stator flux linkage and their actual values. The governing equation for torque for this scheme is due to the interaction of stator and rotor fields. Torque and stator flux linkage are computed from measured motor terminal quantities i.e. stator voltages and current. An optimal voltage vector for the switching of VSI is selected among the six nonzero voltage vectors and two zero voltage vectors by the hysteresis control of stator flux and torque.

As we know from the previous chapter that a three-phase VSI has eight possible combinations of six switching devices which is shown in fig.3.2. The six switches have a well-defined state: ON or OFF in each configuration. So all the possible configurations can be identified with three bits (S_a, S_b, S_c), one for each inverter leg [17]. The bit is set to 1 if the top switch is closed and to 0 when the bottom switch is closed. In order to prevent short circuit of the supply, the state of the upper switch is always opposite to that of the lower one.

The stator voltage space vector is $\bar{V}s = \frac{2}{3} E (S_a + e^{j\frac{2\pi}{3}} S_b + e^{j\frac{4\pi}{3}} S_c)$ (3.1)

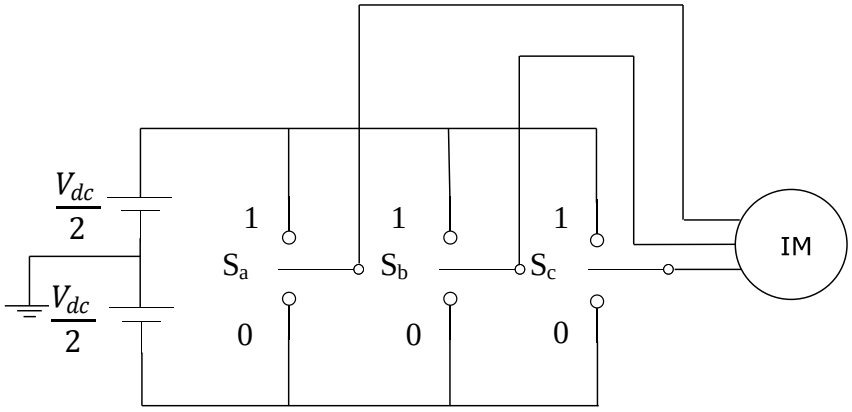

Fig3.2 Simplified 3-ϕ VSI

3.2.1 Direct flux control

In stationary reference frame the stator flux equation can be written as:

$$\bar{\Psi s} = \int (\bar{v}_s - \bar{\imath}_s R_s) dt \quad (3.2)$$

If the stator resistance drop is neglected for simplicity, the stator flux varies along the direction of applied voltage vector and the equation will be reduced to

$$\Delta \bar{\Psi s} = \bar{V}_s \Delta t \quad (3.3)$$

Which means, by applying stator voltage vector $\bar{V}_s$ for a time increment Δt , $\bar{\Psi s}$ can be changed incrementally. The command value of the stator flux vector $\bar{\Psi s}^*$ follows a circular trajectory, the plane of stator flux is divided into six sectors as shown in fig.3.3. Each sector has a different set of voltage vector to increase or decrease the stator flux. The command flux vector rotates in anticlockwise direction in a circular path and the actual stator flux vector $\bar{\Psi s}$ tracks the command flux in a zigzag path but constrained to the hysteresis band which is shown in fig.3.3.

In general the active forward voltage vectors ($V_{s,k+1}$ and $V_{s,k+2}$) are applied to increase or decrease the stator flux respectively when the stator flux lies in sector k. The radial voltage vectors ($V_{s,k}$ and $V_{s,k+3}$) which quickly affect the flux are generally avoided. The active reverse voltage vectors ($V_{s,k-1}$ and $V_{s,k-2}$) are used to increase or decrease the stator flux in reverse direction.

The stator flux vector change due to stator voltage vector is quick whereas change rotor flux is sluggish because of its large time constant T_r. That is why $\bar{\Psi s}$ movement is jerky and $\bar{\Psi r}$

moves uniformly at frequency ω_e as it is more filtered. However the average speed of both remains the same in steady state condition.

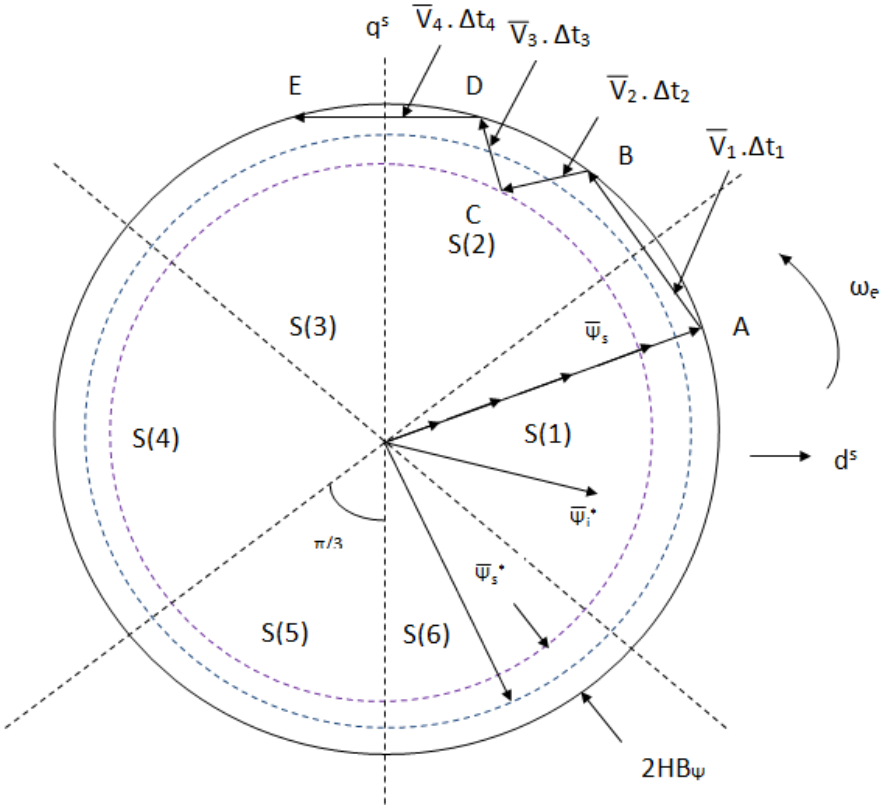

Fig. 3.3 Circular trajectory of stator flux

3.2.2 Direct torque control

The electromagnetic torque produced due to interaction of stator and rotor flux is given by the following equation:

$$T_e = \frac{3}{2}\left(\frac{P}{2}\right)\frac{L_m}{L_s' L_r}\overline{\Psi s} * \overline{\Psi r} = \frac{3}{2}\left(\frac{P}{2}\right)\frac{L_m}{L_s' L_r}\Psi s\ \Psi r \sin\gamma \qquad (3.4)$$

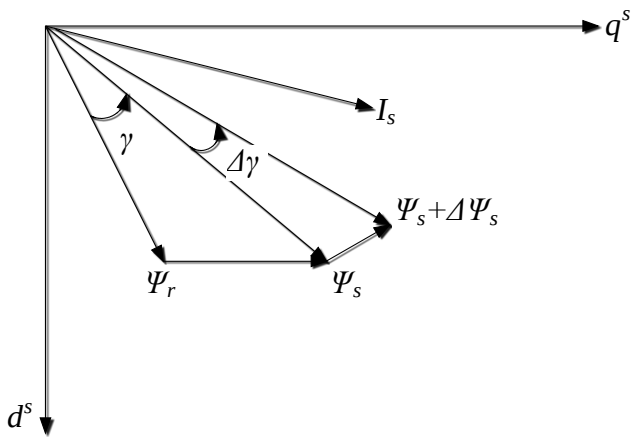

Fig.3.4 Stator flux, rotor flux and stator current vectors in d^s-q^s reference plane

From the above it is clear that torque varies directly as angle between stator flux and rotor flux i.e. γ. So in order to obtain high dynamic performance it is required to vary γ quickly. Assuming the rotor is rotating in anticlockwise direction continuously and stator flux lies in sector k, the active forward voltage vectors ($V_{s,k+1}$ and $V_{s,k+2}$) are applied to increase γ so as the torque T_e. The radial voltage vectors ($V_{s,k}$ and $V_{s,k+3}$) are used to decrease γ and T_e. By applying the reverse active voltage vectors ($V_{s,k-1}$ and $V_{s,k-2}$) torque can be decreased rapidly. The two zero voltage vectors ($V_{s,0}$ and $V_{s,7}$) are applied to maintain the flux constant ideally and to decrease the torque slightly.

3.2.3 Switching selection

A high performance torque control can be established due to the decoupled control of stator flux and torque in DTC. Fig.3.5 shows an example of stator flux located in sector-1 (S(1)) with the corresponding optimum switching voltage vectors for anti-clockwise and clockwise rotation of the shaft.

Optimum switching vector selection table given by table 3.1 shows the optimum selection of the switching vectors in all sectors of the stator flux plane. This table is based on the value of stator flux error status, torque error status and orientation of stator flux for counter-clockwise rotation of the shaft [8].

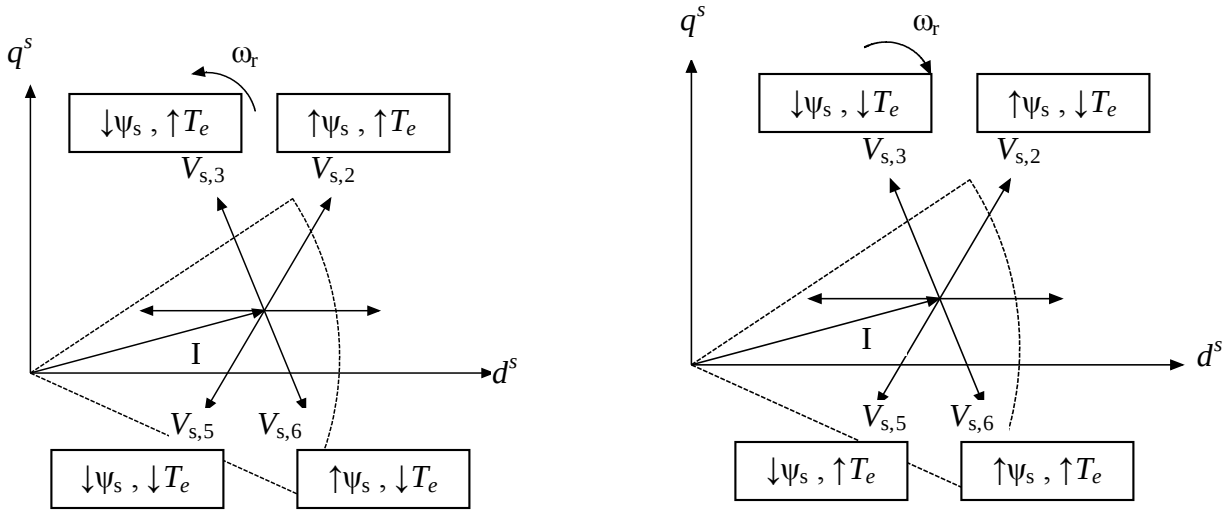

Fig.3.5 Optimum switching voltage vector in sector-1 for (a) anti-clockwise and (b) clockwise rotation

Table 3.1 : Applied selected voltage vectors

$d\psi$	dTe	S(1)	S(2)	S(3)	S(4)	S(5)	S(6)
1	1	V_2	V_3	V_4	V_5	V_6	V_1
	0	V_7	V_0	V_7	V_0	V_7	V_0
	-1	V_6	V_1	V_2	V_3	V_4	V_5
0	1	V_3	V_4	V_5	V_6	V_1	V_2
	0	V_0	V_7	V_0	V_7	V_0	V_7
	-1	V_5	V_6	V_1	V_2	V_3	V_4

3.3 Stator flux estimation

For exact calculation of stator flux and torque errors, an accurate estimator of stator flux is necessary. There are commonly used methods of estimation of flux namely stator voltage model and current model.

3.3.1 Stator voltage model

This is the simplest method of stator flux estimation, where the machine terminal voltages and currents are sensed and from the stationary frame equivalent circuit the fluxes are computed. The estimated stator flux is given by the following equation:

$$\psi_{ds}{}^{s} = \int (v_{ds}^{s} - i_{ds}^{s} R_s)\, dt \quad (3.5)$$

$$\psi_{qs}{}^{s} = \int (v_{qs}^{s} - i_{qs}^{s} R_s)\, dt \quad (3.6)$$

$$\psi_s = \sqrt{\psi_{ds}^{s2} + \psi_{qs}^{s2}} \quad (3.7)$$

This method provides accurate flux estimation at high speed but in industrial applications requiring vector drives at zero start-up this method cannot be used because at low speed stator resistance drop becomes significant causing inaccurate estimation. Also at low frequency, voltage signals are very low and dc offset tends to build up at the integration output, as a result ideal integration becomes difficult.

3.3.2 Current model

In stationary reference frame, current model is globally stable and the drives operation can be extended down to zero speed. But this model is much complex as compared to voltage model as here the knowledge of rotor speed and stator current is required to estimate rotor flux linkage and stator flux can be estimated based on the estimation of rotor flux linkage. From the dynamic equations of IM in stationary reference frame, stator and rotor flux can be derived which are given below:

$$\frac{d}{dt}\bar{\psi}r = ((L_m i_s - \bar{\psi}r)/Tr) - \omega_r \psi_r \quad (3.8)$$

$$\bar{\Psi_s} = \frac{L_m}{L_r}\bar{\psi}r + \sigma L_s i_s \quad (3.9)$$

Here the equations involve closed loop integration, so there is no integration drift problem in current model at low speed region. However estimation accuracy is affected due to motor parameter variation, particularly rotor resistance variation becomes dominant by skin effect and temperature.

It is ideal to have a hybrid model based on the unique features gained by both models respectively where the voltage model would be effective at higher speed range and current model at lower speed range.

3.4 Hysteresis controller

DTC of induction motor drives requires two hysteresis controllers. The drive performance is influenced by the width of the hysteresis bands in terms of flux and torque ripples, current harmonics and switching frequency of power electronics devices. Current distortion is reduced by small flux hysteresis band and torque ripple is reduced by small torque hysteresis bands. In each sampling time, the switching state of the inverter is updated. The inverter state remains constant, until the output states of the hysteresis controller change within a sampling interval. If the hysteresis band is fixed, the switching frequency totally depends on the rate of change of torque and flux.

3.4.1 Torque hysteresis controller

The Torque hysteresis controller is a three level controller. It means the torque control loop has three levels of digital outputs. The torque error ΔT_e is given to the torque hysteresis controller and the output is torque error status (dT_e) which can have three values -1, 0 or 1. The width of the hysteresis band is $2\Delta T_e$. Torque error status is given to the switching table for optimum voltage vector selection for the inverter.

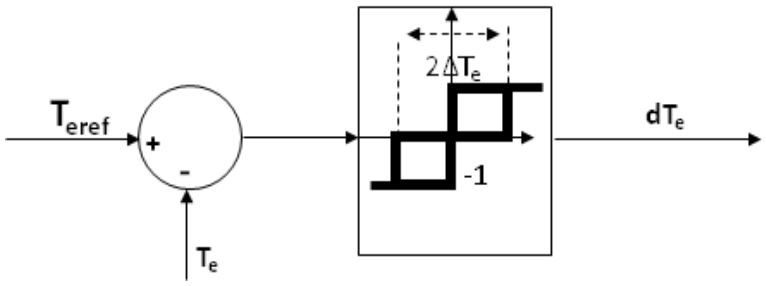

Fig.3.6 (a) Torque hysteresis controller

Torque error $\Delta T_e = T_{eref} - T_e$

$|dTe| = 1$ if $|Te| < |Teref| - |\Delta Te|$: Torque to be increased

$|dTe| = -1$ if $|Te| > |Teref| + |\Delta Te|$: Torque to be decreased

$|dTe| = 0$ if $|Teref| - |\Delta Te| \leq |Te| \leq |Teref| + |\Delta Te|$: Torque to remain unchanged

3.4.2 Flux hysteresis controller

The flux hysteresis controller is a two level controller. So the flux control loop has two digital outputs. The stator flux error $\Delta\psi_s$ is given to the flux hysteresis controller and the output is flux error status ($d\psi_s$) which can have two values 0 and 1. The width of the hysteresis band is $2\Delta\psi_s$. Flux error status is given to the switching table for optimum voltage vector selection for the inverter.

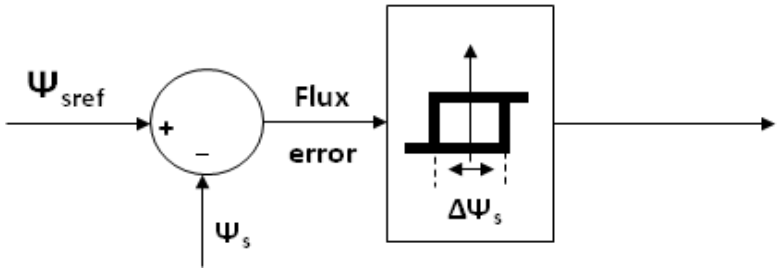

Fig.3.6 (b) Flux hysteresis controller

Stator flux error $\Delta\psi_s = \psi_{sref} - \psi_s$

The flux is controlled according to the following equations

$|d\psi_s| = 1$ if $|\psi_s| \leq |\psi_{sref}| - |\Delta\psi_s|$:flux to be increased

$|d\psi_s| = 0$ if $|\psi_s| \geq |\psi_{sref}| + |\Delta\psi_s|$: flux to be decreased

3.5 Indirect Field oriented control

In indirect vector control the unit vectors ($\cos\theta_e$ *and* $\sin\theta_e$) are generated in feed forward manner. As shown in the fig. d^s-q^s axes is fixed in the stator, d^r-q^r axes rotating at rotor speed ω_r, synchronously rotating axes d-q are rotating ahead of d^r-q^r by slip angle $\theta_{sl,}$. Rotor field is directed along *d*-axis, $\omega_e = \omega_r + \omega_{sl}$, so

$$\theta_e = \int \omega_e \, dt = \int (\omega_r + \omega_{sl}) \, dt = \theta_r + \theta_{sl} \qquad (3.10)$$

The rotor circuit equations in d-q equivalent circuit can be written as:

$$\frac{d}{dt}\psi_{dr} + R_r \, i_{dr} - (\omega_e - \omega_r)\,\psi_{qr} = 0 \qquad (3.11)$$

$$\frac{d}{dt}\psi_{qr} + R_r \, i_{qr} + (\omega_e - \omega_r)\,\psi_{dr} = 0 \qquad (3.12)$$

$$\psi_{dr} = L_r\, i_{dr} + L_m\, i_{ds} \tag{3.13}$$

$$\psi_{qr} = L_r\, i_{qr} + L_m\, i_{qs} \tag{3.14}$$

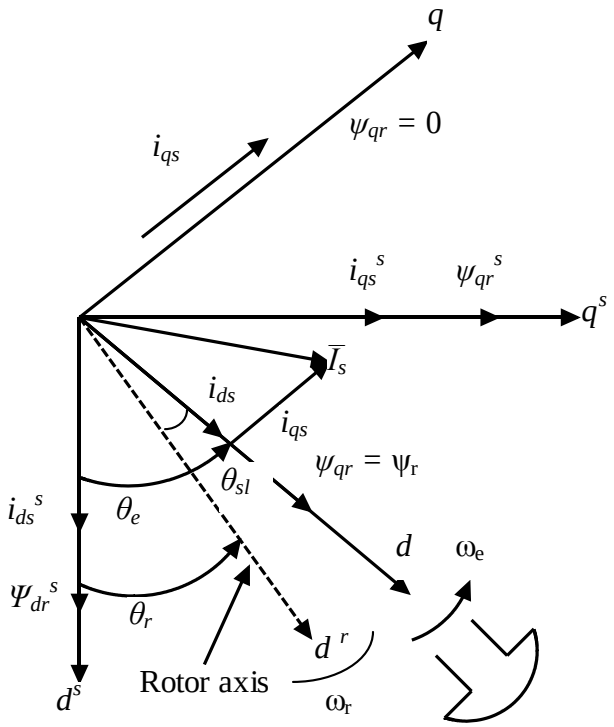

Fig.3.7 Phasor diagram explaining indirect Field oriented control

For decoupling control $\psi_{qr} = 0$, so $\psi_{dr} = \psi_r$

Solving all the above eq. we get $\psi_r = \frac{L_m\, i_{ds}}{(1+s\,T_r)}$ (3.15)

At steady state, the rotor flux is proportional to current i_{ds}.

3.5 Conclusion

This chapter included the detail description of the conventional DTC scheme and principle of indirect FOC scheme. This DTC scheme has many advantages over field oriented control which has been discussed in this chapter but also has some drawbacks like generation of flux and torque ripple and variable switching frequency. The flux and torque ripple is due to the hysteresis controller which can however be reduced significantly by reducing the sampling period. The variable switching frequency is due to sector change of the stator flux vector.

CHAPTER-4

SPACE VECTOR PULSE WIDTH MODULATION FED INDUCTION MOTOR DRIVES

4.1 Introduction

The use of PWM drive is advantageous in many ways, for example it obtains its dc input through uncontrolled rectification of commercial AC mains and has good power factor, good efficiency, relatively free from regulation problems, it has the ability to operate the motor with nearly sinusoidal current waveform. The conventional PWM techniques are suitable for open loop control, for the implementation of a closed loop controlled AC drive Space vector PWM (SVPWM) technique is applied. In this technique, the switching patterns for the bridge inverter are generated from the knowledge of stator voltage space phasor. A reference voltage vector is generated to generate a field synchronous with the rotating voltage vector by utilizing the different switching states of a three phase bridge inverter [18].

4.2 Theory of Space vector pulse width modulation

When three phase supply is given to the stator of the induction machine, a three phase rotating magnetic field is produced. Due to this field flux, a three phase rotating voltage vector is generated which lags the flux by 90º. This field can also be realized by a logical combination of the inverter switching which is the basic concept of SVPWM.

4.2.1 Realization of voltage space phasor

The three phase bridge inverter has eight possible switching states: six active and two zero states. The six switches have a well-defined state ON or OFF in each configurations. At a particular instant, only one switch in each of the three legs is ON. Corresponding to each state of the inverter, there is one voltage space vector. For example for state zero it is V_0, for state 1 it is V_1 and so on. These switching state vectors have equal magnitude but 60º apart from each other [8]. These vectors can be written in generalized form as follows:

$$V_k = V_{dc} e^{j(\frac{k-1}{3})\pi} \qquad k = 1, 2, \ldots\ldots, 6$$
$$= 0 \qquad k = 0, 7 \qquad (4.1)$$

Where k = inverter state number.

V_{dc} = dc link voltage of the inverter

The inverter state vectors can be drawn as shown in fig.4.1

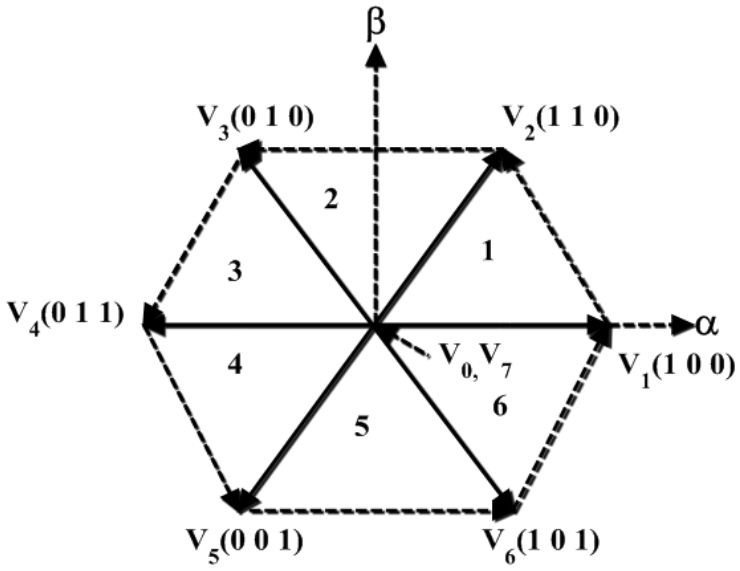

Fig.4.1 Inverter switching state vectors

The space bounded by two inverter space vectors is called a sector. So the plane is divided into six sectors each spanning 60º. In a balanced three phase system the voltage vectors are 120º apart in space and are represented by rotating vectors, whose projections on the fixed three phase axes are, sinusoidal waves. So they can be represented as three sinusoidal references by a voltage reference space vector V_{ref}^* or V_s^*. The reference vector is assumed to be rotating in counter-clockwise direction with respect to d^s-axis (α-axis) as shown in fig.4.2 through six sectors.

The reference space vector can be synthesized by a combination of eight state vectors and is constant in magnitude at a switching instant t_s in case the switching frequency much higher than the output frequency. In a time average sense the reference vector at that instant can be approximated by two active voltage states of the inverter. For only certain amount of time these states are valid.

$$V_s^* = V_k t_k + V_{k+1} t_{k+1} \qquad k = 0, 1, 2\ldots\ldots, 7 \qquad (4.2)$$

In SVPWM, it is assumed that the space phasor of stator voltage V_s^*, is moving in α-β plane with constant angular velocity describing approximately a circular path. The basis of SVPWM scheme is to sample the V_s^* at sufficiently high rate, in between the sampling instants the vector is assumed to be constant in magnitude as shown in fig.4.2.

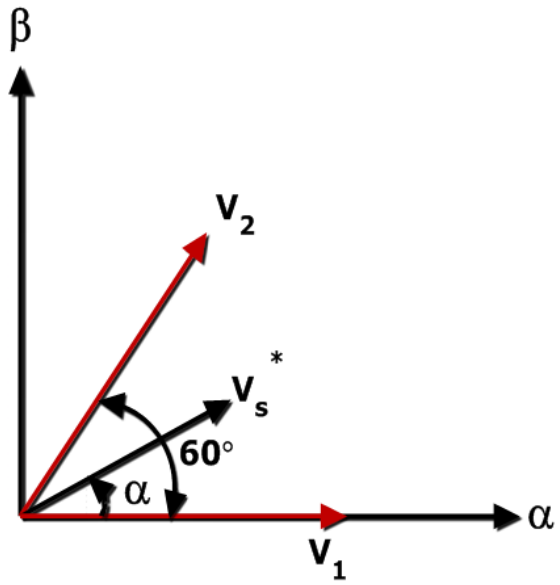

Fig.4.2 Reference vector in sector 1

In sector 1, the space voltage vector V_1 is along α-axis, V_2 makes an angle 60º to V_1 and at a particular instant V_s^* is making an angle γ w.r.t V_1. To generate the reference space vector in sector 1, the switching state vector V_1 is applied for an interval t_1, V_2 for t_2 and the two zero vectors V_0, V_7 for interval t_0, t_7[16] respectively. So the total sampling interval t_s can be written as:

$$t_s = t_1 + t_2 + t_0 + t_7 \qquad (4.3)$$

Resolving V_s^* and V_1, V_2 along the α-β axis, and by equating voltage-time integrals we get:

$$|V_s^*|\, t_s \cos\gamma = |V_1|\, t_1 + |V_2|\, t_2 \cos\frac{\pi}{3} \qquad (4.4)$$

$$|V_s^*|\, t_s \sin\gamma = |V_2|\, t_2 \sin\frac{\pi}{3} \qquad (4.5)$$

Dividing both sides of equation (4.4) and (4.5) by V_{dc} and substituting $abs\left(\frac{V_s^*}{V_{dc}}\right)$ = a, we get:

$$a t_s \sin\gamma = \frac{\sqrt{3}}{2} t_2$$

$$\text{or} \quad t_2 = (2\, a\, t_s \sin\gamma) / \sqrt{3} \qquad (4.6)$$

$$\text{and} \qquad a\, t_s \cos\gamma = t_1 + \frac{1}{2}t_2 \tag{4.7}$$

Substituting the value of t_2 from equation (4.6) in (4.7) and multiplying both sides of resulting equation by $\frac{\sqrt{3}}{2}$, we obtain

$$t_1 = \frac{2\,a\,t_s}{\sqrt{3}} \sin\left(\frac{\pi}{3} - \gamma\right) \tag{4.8}$$

$$t_0 = t_7 = t_s - (t_1 + t_2) \tag{4.9}$$

Where a = modulation index = $abs\left(\frac{V_s^*}{V_{dc}}\right)$

By the knowledge of t_0, t_1, t_2, t_7 , the switching pattern can be determined if the vector is in sector 1. The four time intervals change simultaneously when V_s^* goes from one sector to another for a particular modulation index a. The full cycle is completed by six similar sectors with label 1, 2,….,6. As V_s^* move over to sector 2, the inverter remains in switching state vector V_2 for time interval t_1 and in V_3 for time t_2. For sector 3: V_3 for t_1 and V_4 for t_2 and so on.

4.2.2 Pulse pattern generation

The PWM pattern generation means the generation of gating pulses for the six switches of the inverter, for correct interval so that appropriate switching state vectors are active for the appropriate time intervals as the reference space vector moves over a full cycle.

In order to obtain minimum switching frequency, it is desired that only one phase of the inverter changes state from $+\frac{V_{dc}}{2}$ to $-\frac{V_{dc}}{2}$ while changing the switching vectors. So the arrangement of the switching sequence should be such that the transition from one state to the next state is performed by switching only one inverter phase. This is done by switching the inverter legs in a sequence starting from one zero state and ending at another zero state. Fig.4.3 shows the optimum inverter phase to dc center tap voltages. It can be noted that the switching frequency of the inverter is half of the sampling frequency [8] [14].

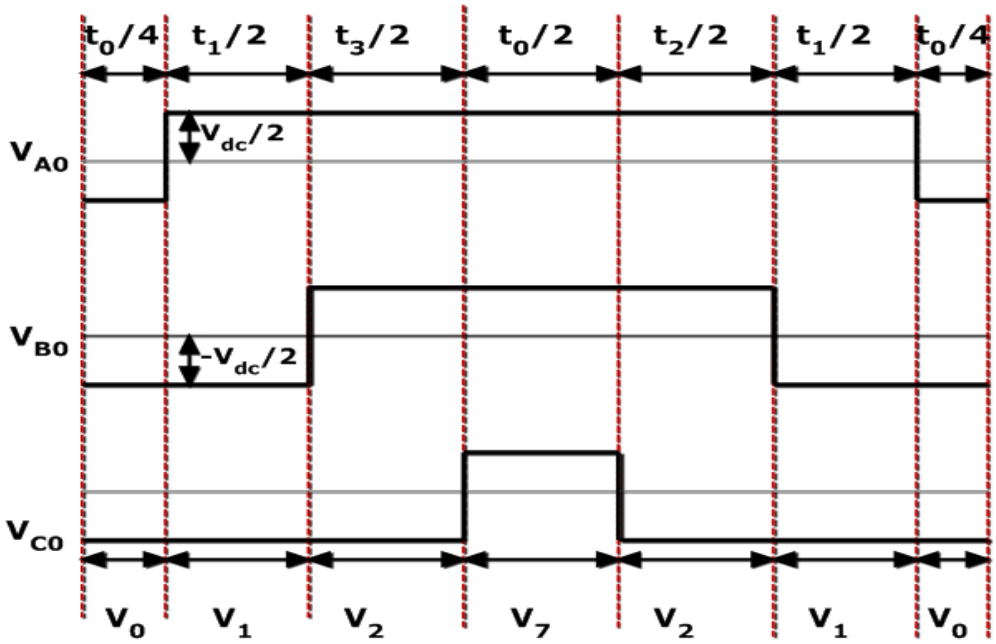

Fig.4.3 Leg voltages and space vector disposition in sector 1

The mean values of the phase to center tap voltages (V_{A0}, V_{B0}, V_{C0}) can be evaluated, averaging over one sampling period t_s as follows:

$$\bar{V}_{A0} = \frac{V_{dc}}{2t_s}\left(-\frac{t_0}{2} + t_1 + t_2 + \frac{t_0}{2}\right) \quad (4.10)$$

$$\bar{V}_{B0} = \frac{V_{dc}}{2t_s}\left(-\frac{t_0}{2} - t_1 + t_2 + \frac{t_0}{2}\right) \quad (4.11)$$

$$\bar{V}_{C0} = \frac{V_{dc}}{2t_s}\left(-\frac{t_0}{2} - t_1 - t_2 + \frac{t_0}{2}\right) \quad (4.12)$$

Substituting the values of t_1, t_2 in above three equations

$$\bar{V}_{A0} = \frac{a\,V_{dc}}{\sqrt{3}}\sin\left(\gamma + \frac{\pi}{3}\right) \quad (4.13)$$

$$\bar{V}_{B0} = a\,V_{dc}\sin\left(\gamma - \frac{\pi}{6}\right) \quad (4.14)$$

$$\bar{V}_{C0} = -\,\bar{V}_{A0} \quad (4.15)$$

4.4 Conclusion

The mean value of the phase voltages obtained by SVPWM technique has triple harmonics which is eliminated in line voltage. The peak value of the line voltage is 15% more than that in sine PWM at maximum modulation index, so this method of PWM generation gives better utilization of dc bus voltage for inverter.

CHAPTER-5

SIMULATION MODELS, RESULTS AND DISCUSSIONS

5.1 Simulation model of IM

The three phase induction motor model is simulated by using the Matlab/Simulink. Using the set of equations provided in chapter 2, the Model is implemented. Figure 5.1 depicts the complete Simulink model of IM. The performance of the motor is first checked out for no load condition and then the load torque of 2Nm is applied and performance characteristics are drawn. The specification of the IM used is 1.5KW, 1440 rpm, 4 pole, 3-phase with parameters: R_s = 7.83 ohm, R_r= 7.55 ohm, L_s= L_r = 0.4751 H, L_m= 0.4535 H, J= 0.06 Kg.m^2, B= 0.01 Nm.sec/rad.

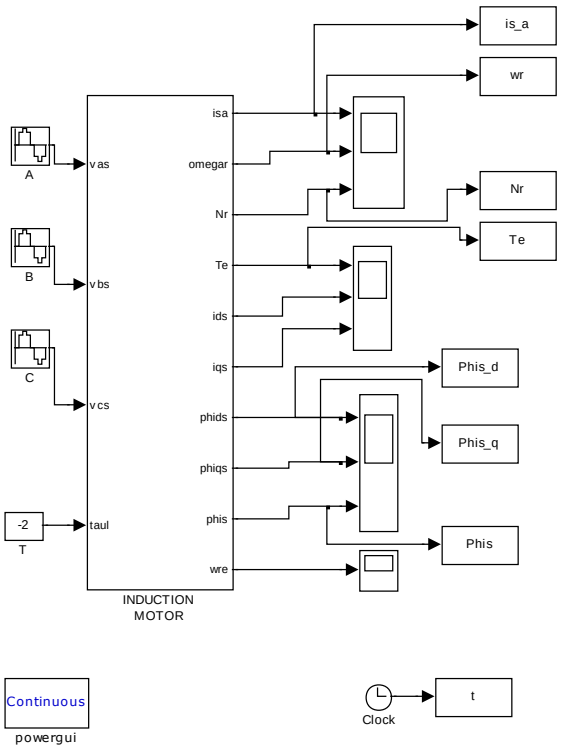

Fig.5.1 Simulation model of IM

Results for no load condition, (T_L = 0)

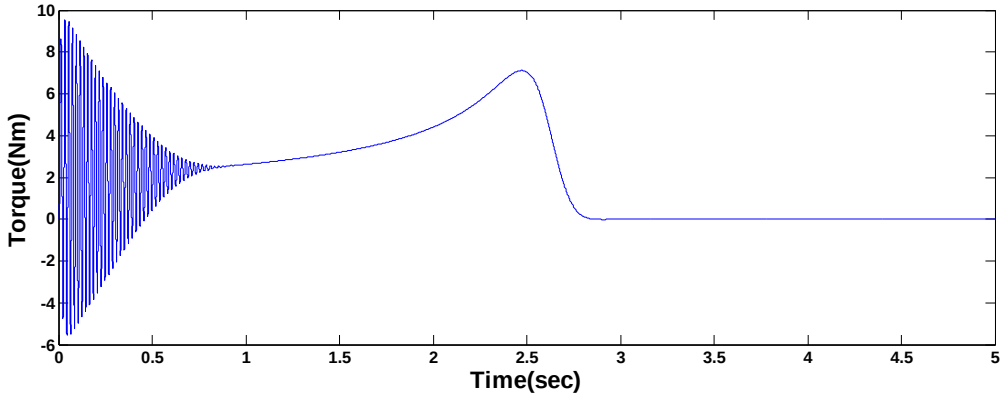

Fig.5.2 (a) Electromagnetic torque

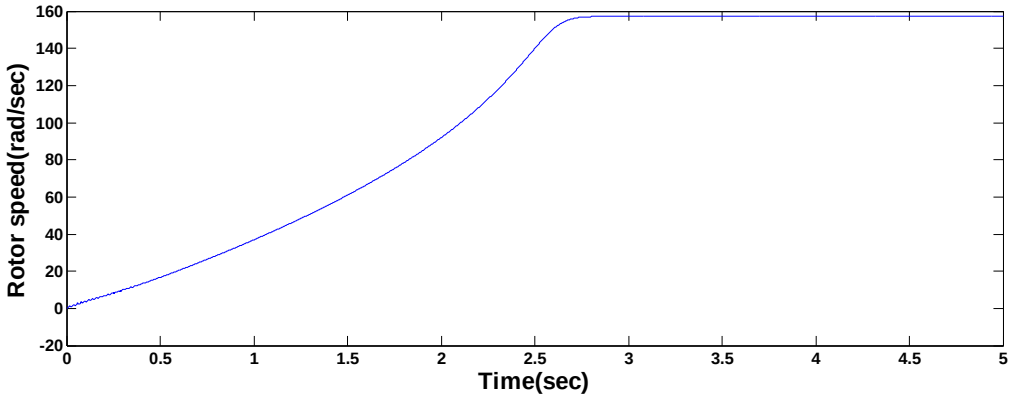

Fig.5.2(b) Rotor speed

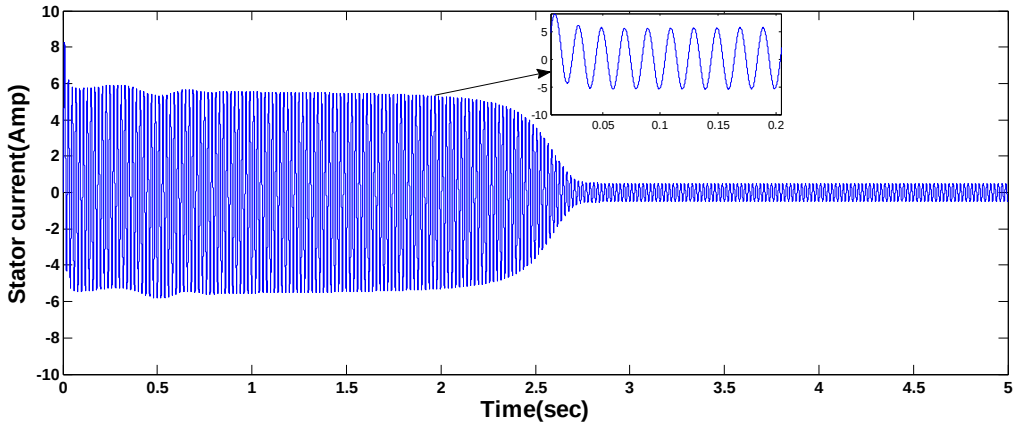

Fig.5.2(c) Stator current

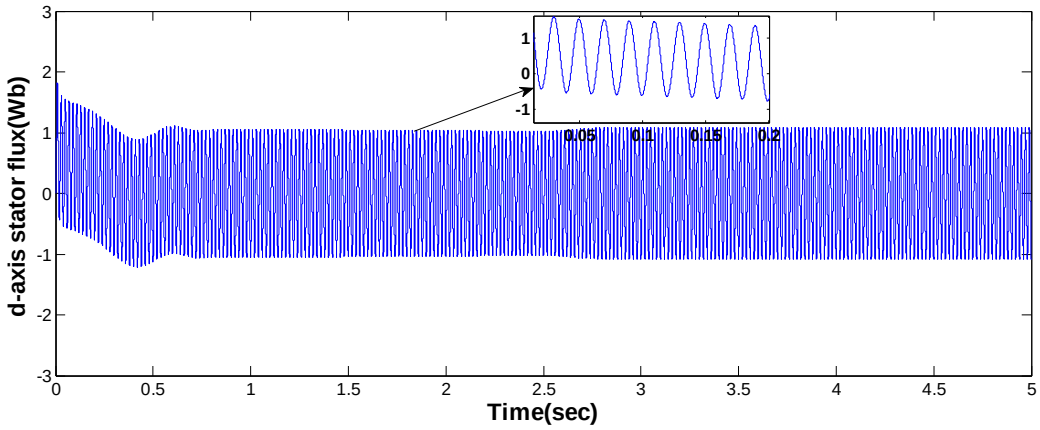

Fig.5.2 (d) d-axis stator flux

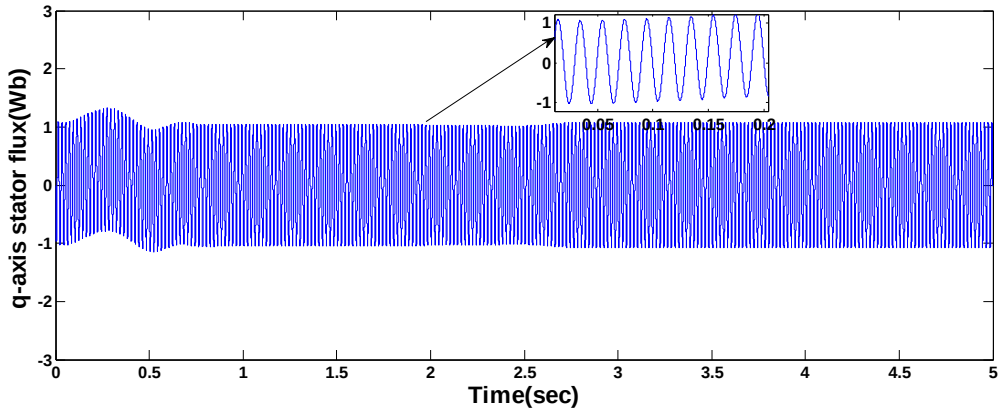

Fig.5.2 (e) q-axis stator flux

For T_L = 2 Nm

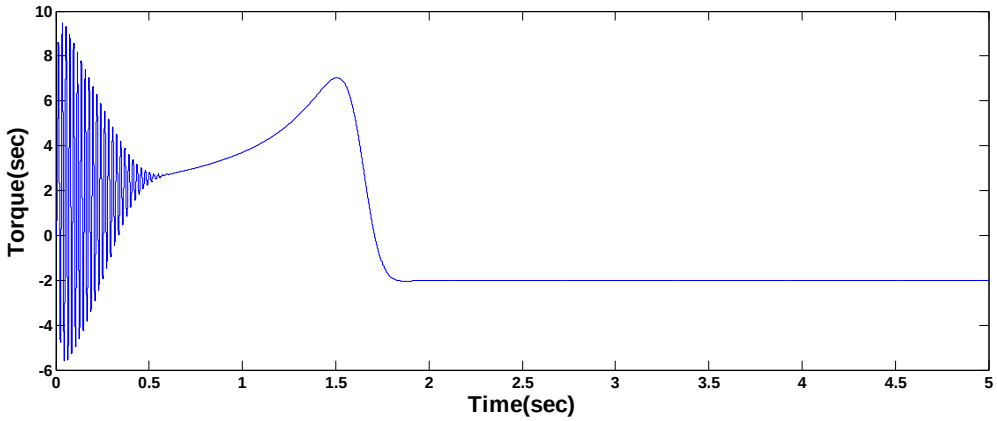

Fig.5.3 (a) Electromagnetic torque

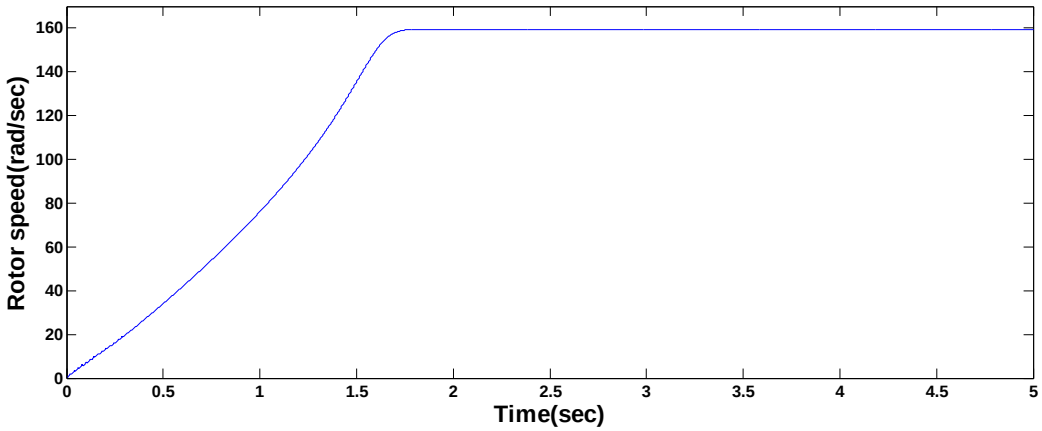

Fig.5.3 (b) Rotor speed

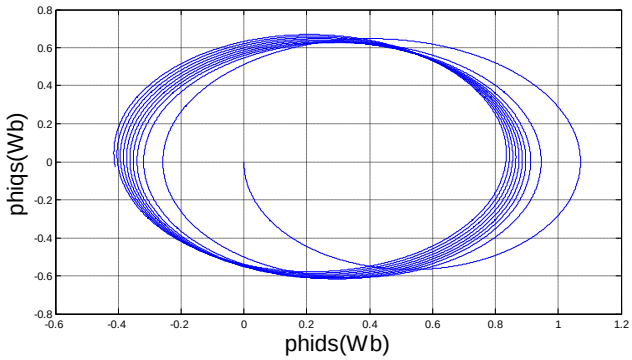

Fig.5.4 Trajectory of d axis and q axis stator flux in stationary reference frame

6.2 Simulation of DTC scheme

A direct torque control algorithm of Induction motor drive has been simulated using Matlab/Simulink. The reference flux linkage is taken as 1 V.s and load torque applied is 200N-m.The motor is fed from an IGBT PWM inverter (Universal bridge). The MATLAB/ SIMULINK model for switching logic is developed. The transient performance of the developed DTC model has been tested by applying a load torque command on the mechanical dynamics. The model is run for typical conditions of reference speed and applied torque value. Figure 5.2 depicts the complete Simulink model of DTC scheme of IM.A 50HP, 460V, 60Hz, 4pole, 3-phase induction motor is used for the simulation. The parameters of the IM are given in appendix A.

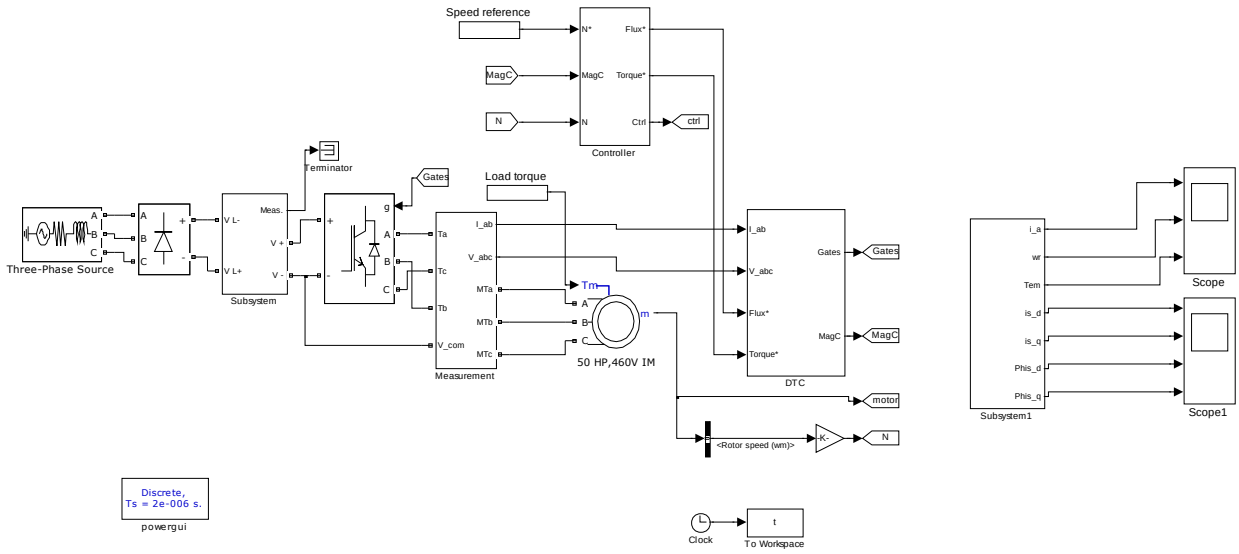

Figure 5.5 Simulink model of DTC scheme of IM

Result and discussion

Figure.5.6 shows the results obtained. Figure 5.6(a) shows the electromagnetic torque and Figure 5.6(b) shows the rotor speed of the machine. This demonstrates that the developed DTC achieved high dynamic performance in speed response to changes in demand torque. However, there is some performance degradation with torque overshoot in the torque transient owing to the hysteresis controllers used. Figure 5.6(c) and (d) show the d and q axis stator flux magnitude, emphasizing the decoupled action of torque and flux control. It is observed that the variation of motor torque does not influence fluxes. Figure 5.6(e) and (f) show d and q axis stator currents.

Fig 5.6(a) and (b) show the motor electromagnetic torque and rotor speed. The torque has high initial value in the acceleration zone, increases due to load torque increment then decreases and remains constant in the deceleration zone. Fig.5.6(c) shows that at first flux increases in transient period and then it comes to steady state so that flux is maintained constant to control the torque. The q-axis stator flux varies with torque; it has high initial value in the acceleration zone then decreases and comes to steady state.

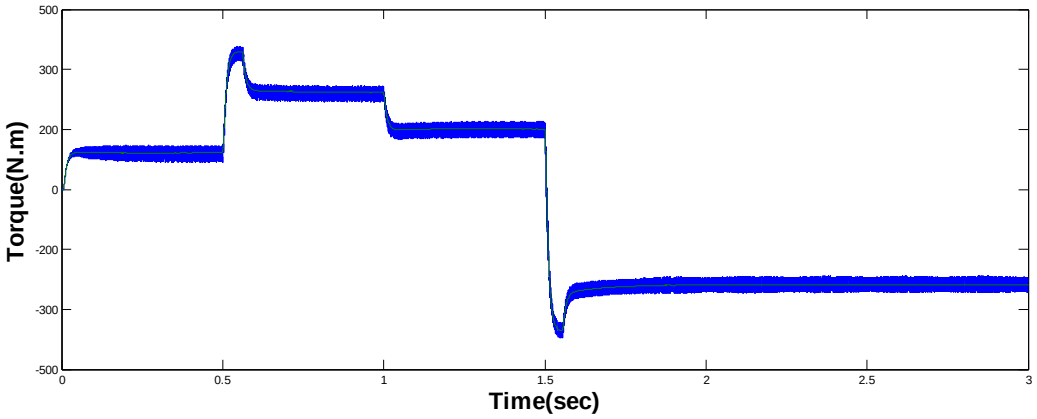

Fig.5.6 (a) Electromagnetic torque

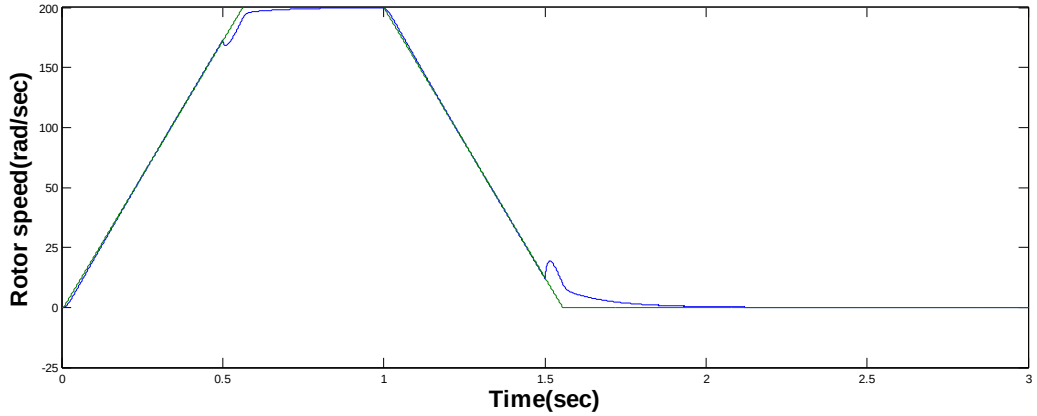

Fig.5.6 (b) Rotor speed

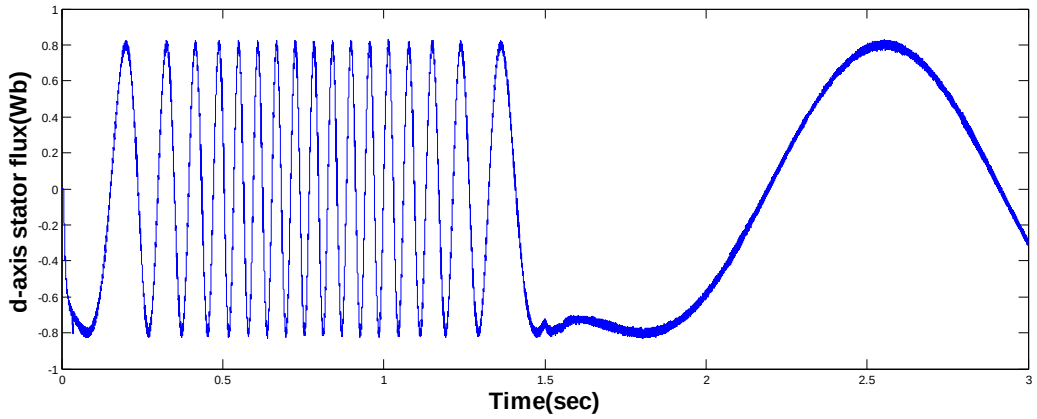

Fig.5.6 (c) d-axis stator flux

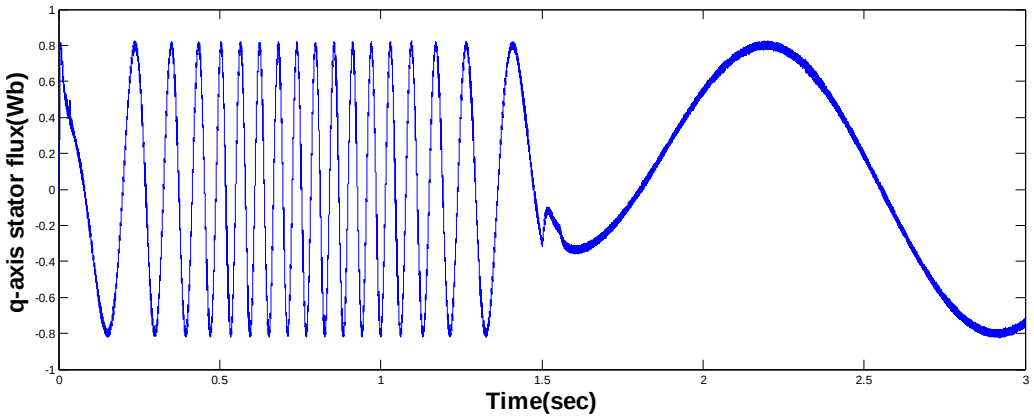

Fig.5.6 (d) q-axis stator flux

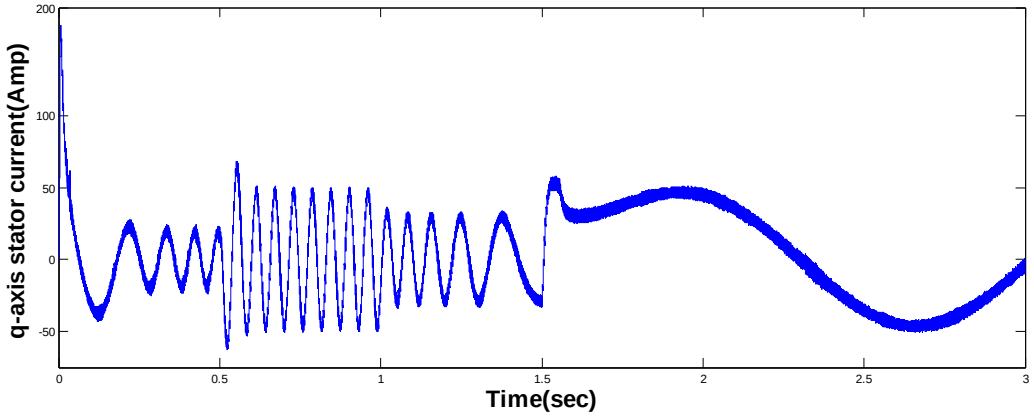

Fig.5.6(e) d-axis stator current

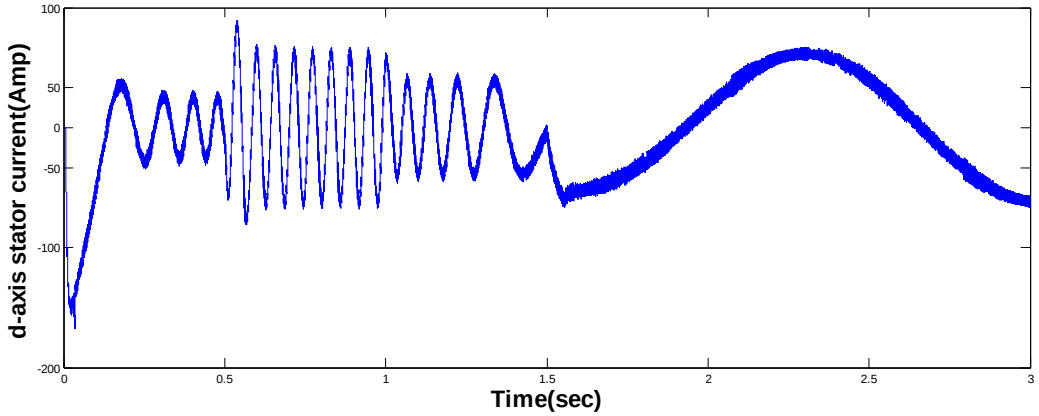

Fig.5.6 (f) q-axis stator current

Results of SVPWM based FOC scheme

Fig 5.7(a) and (b) show the mean value of inverter output voltages by SVPWM. Fig.5.7(c) and (d) show the motor torque and rotor speed in case of FOC based on SVPWM. The torque has high initial value in acceleration zone then decreases in constant speed region, again

increases due to increment in load torque and remains constant at a high value in further acceleration zone to next speed set point.

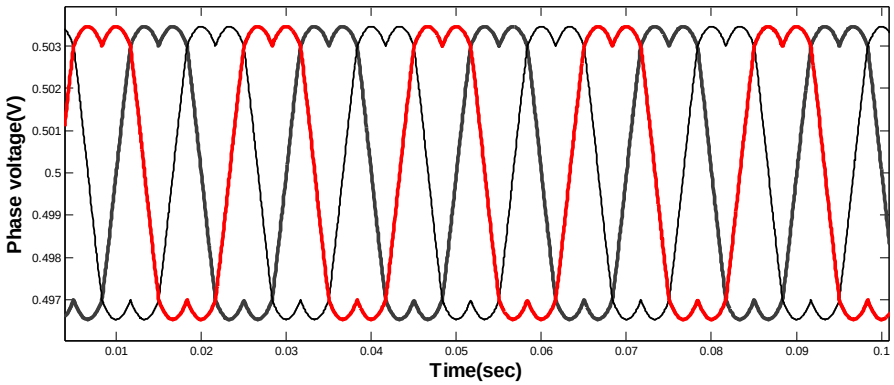

Fig.5.7 (a) Mean value of Phase voltage of inverter

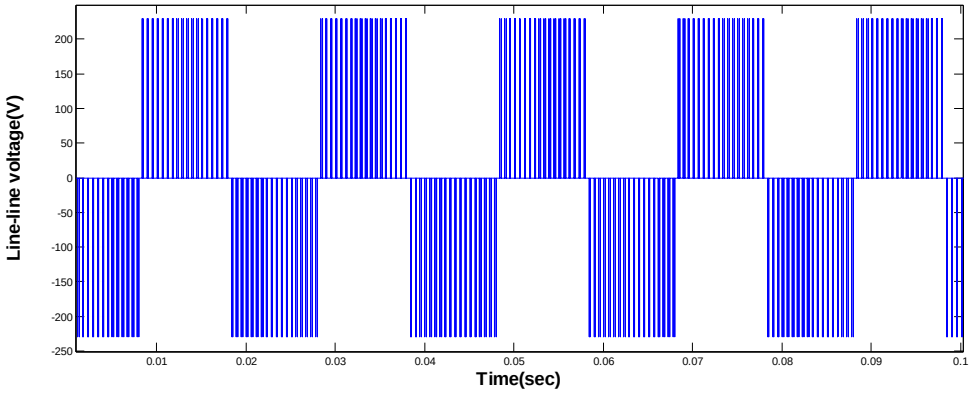

Fig.5.7 (b) Line voltage output of inverter

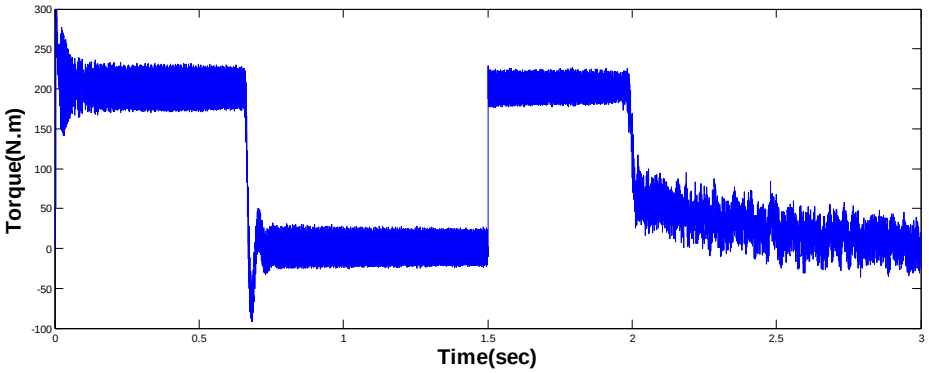

Fig.5.7 (c) Electromagnetic torque

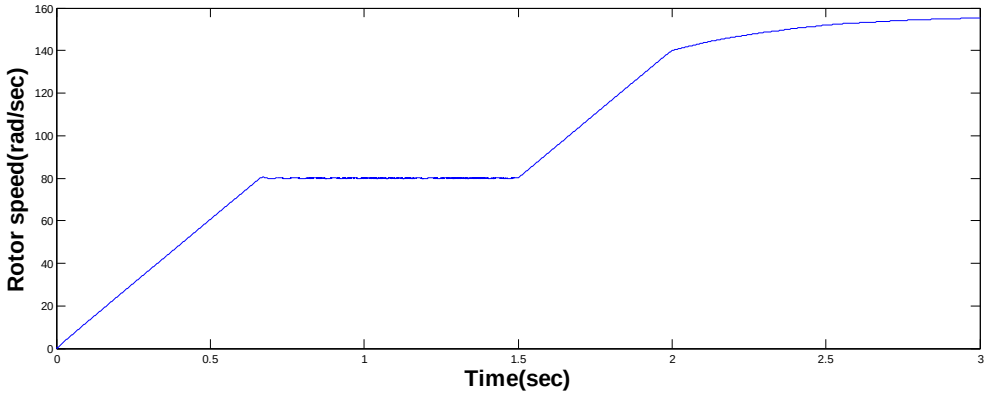

Fig.5.7 (d) Rotor speed

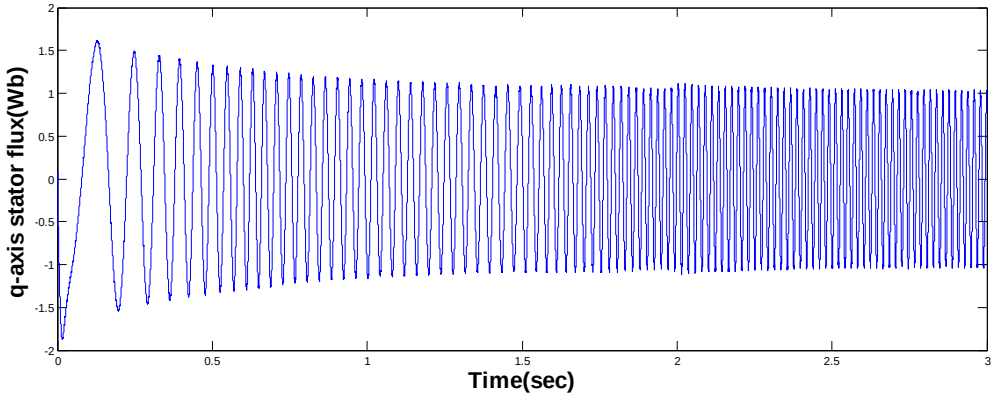

Fig.5.7 (e) q-axis stator flux

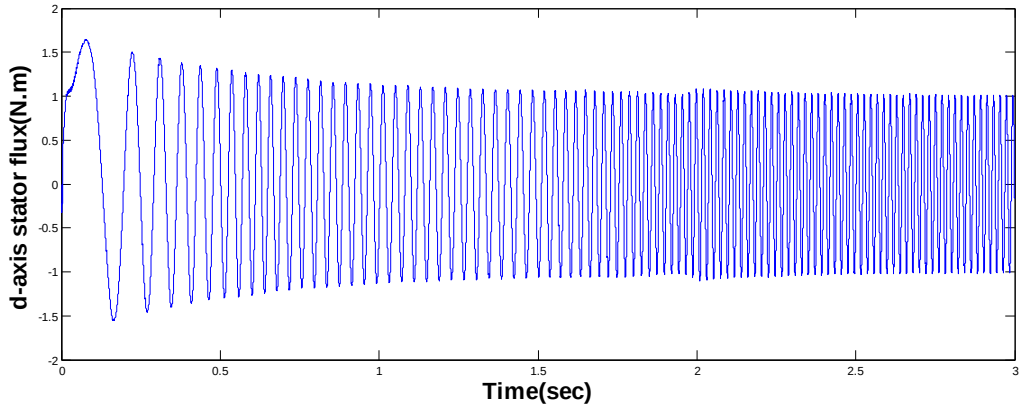

Fig.5.7 (f) d-axis stator flux

CHAPTER-6

CONCLUSIONS AND FUTURE WORKS

6.1 Summery and conclusions

For any IM drives, Direct torque control is one of the best controllers proposed so far. It allows decoupled control of motor stator flux and electromagnetic torque. From the analysis it is proved that, this strategy of IM control is simpler to implement than other vector control methods as it does not require pulse width modulator and co-ordinate transformations. But it introduces undesired torque and current ripple.

DTC scheme uses stationary *d-q* reference frame with *d*-axis aligned with the stator axis. Stator voltage space vector defined in this reference frame control the torque and flux. The main inferences from this work are:

1. In transient state, by selecting the fastest accelerating voltage vector which produces maximum slip frequency, highest torque response can be obtained.
2. In steady state, the torque can be maintained constant with small switching frequency by the torque hysteresis comparator by selecting the accelerating vector and the zero voltage vector alternately.
3. In order to get the optimum efficiency in steady state and the highest torque response in transient state at the same time, the flux level can be automatically adjusted.
4. If the switching frequency is extremely low, the control circuit makes some drift which can be compensated easily to minimize the machine parameter variation.

The estimation accuracy of stator flux is very much essential which mostly depends on stator resistance because an error in stator flux estimation will affect the behavior of both torque and flux control loops. The torque and current ripple can be minimized by employing space vector modulation technique.

6.2 Future Scope of work

In conventional DTC scheme, high torque ripple is produced because the selected voltage space vector is applied for the entire switching period irrespective of the magnitude of the torque error. This torque ripple can be minimized in order to achieve a better drive performance, by varying the duty ratio of the selected voltage vector during each switching period, based on the magnitude of the torque error and position of the stator flux. This constitutes the basic of SVPWM technique. So the future work is to simulate DTC scheme based on SVPWM technique and to have comparative study of conventional DTC scheme and DTC-SVM scheme.

REFERENCES

[1] B. K.Bose. 1997. Power Electronics and Variable Frequency Drives. IEEE Press, New York.

[2] Kazmierkowski, R.Krishnan, Blaabjerg, Control in Power Electronics, Selected Problems.

[3] Takahashi Isao, Noguchi Toshihiko, ''A New Quick-Response and High-Efficiency Control Strategy of an Induction Motor'', *IEEE Transactions on Industry Applications*, Vol. IA-22 No-5, Sept/Oct 1986.

[4] Thomas G.Habetler, Francesco Profumo, Michele Pastorelli and Leon M. Tolbert "Direct Torque Control of IM using Space Vector Modulation" *IEEE Transactions on Industry Applications*, Vol.28, No.5, Sept/Oct 1992.

[5] E.Bassi, P. Benzi, **S.** Buja, "**A** Field Orientation Scheme for Current-Fed Induction Motor Drives Based on the Torque Angle Closed-Loop Control" *IEEE Transactions on Industry Applications*, Vol. 28, No. 5, Sept./ Oct. 1992.

[6] James N. Nash, "Direct Torque Control, Induction Motor Vector Control Without an encoder" *IEEE Trasaction on Industry applications*,Vol.33,No.2,March/April 1997.

[7] M. Depenbrock, ''Direct Self-Control (DSC) of Inverter-Fed Induction Machine'', *IEEE Transactions on Power Electronics*, Vol.3, No.4, Oct.1988.

[8] Cristian Lascu, Boldea, Blaabjerg "A Modified Direct Torque Control for Induction Motor Sensorless Drive" *IEEE transaction on Industry Applications*, Vol.36, No.1, Jan/Feb 2000.

[9] Anthony Purcell, P. Acarnley, "Enhanced Inverter Switching for Fast Response Direct Torque Control" *IEEE Transactions on Power Electronics*, Vol. 16, No. 3, may 2001.

[10] M.Vasudevan, R.Arumugam "New Direct Torque Control Scheme of Induction Motor for Electric vehicle" *Proceeding of control conference,5th Asian*,Vol.2, 2004.

[11] M.Vasudevan, R.Arumugam, S.Paramasivam" High performance adaptive Intelligent DTC Schemes for induction motor drives" *SJEE*, Vol.2, No1,May 2005.

[12]Sarat K. Sahoo, G. Tulsi Ram Das, Vedam Subrahmanyam "Implementation and Simulation of DTC scheme with the use of FPGA scheme" *ARPN Journal of Engineering and Applied Sciences*, Vol.3. No.2, April 2008.

[13] Ehsan Hassankhan, Davood A. Khaburi,"DTC-SVM Scheme for Induction Motors Fed with a Three-level Inverter", *World Academy of Science, Engineering and Technology* 2008.

[14] L. Bouras, M. Kadjoudj, "Vector control of induction motor based Space Vector Modulation" *Electronics and Telecommunications,* Vol.50, No.1, 2009.

[15] Prof.K.B.Mohanty "A Direct Torque Controlled Induction Motor with Variable Hysteresis Band" 11th *International Conference on Computer Modelling and Simulation,* UK Sim 2009.

[16] Zhifeng Zhang, Renyuan Tang, "Novel Direct Torque Control Based on Space Vector With Modulation Adaptive Stator Flux Observer for Induction Motors" *IEEE Transactions on Magnetics*, Vol. 46, No. 8, August 2010.

[17] T.Nasser et al, "direct torque control of induction motor based on artificial neural networks With estimate and regulation speed using the MRAS and neural pi controller" Journal of Theoretical and Applied Information Technology" 2010.

[18] S Allirani, V Jagannathan, "High Performance Direct Torque Control of Induction Motor Drives Using Space Vector Modulation" IJCSI, Vol. 7, Issue 6, November 2010.

[19] K. Kaur, S. Duvvuri, S. Singh, "Simulation of Indirect Vector Controlled Induction Motor Drive" *IEEE International Conference on Advanced Computing & Comm.Techno.*2011.

[20] Giovanna Oriti and Alexander L. Julian,"Three-Phase VSI with FPGA-Based Multisampled Space Vector Modulation" *IEEE transactions on industry applications*, Vol. 47, No. 4, July/August 2011.

[21] AuzaniJidin, NikIdris, Mohamed Yatim, "Simple Dynamic Overmodulation Strategy For Fast Torque Control in DTC of Induction Machines With Constant-Switching-Frequency Controller"*IEEE transactions on industry applications*, Vol. 47, No. 5, Sept/Oct 2011.

[22]A. Mishra, P.Choudhary, "Speed Control Of An Induction Motor By Using Indirect Vector Control Method" *IJETAE*,Volume 2, Issue 12, December 2012.

[23] H. Arabaci and O. Bilgin, "Squirrel Cage of Induction Motors Simulation via Simulink" *International Journal of Modeling and Optimization,* Vol. 2, No. 3, June 2012.

[24] Sifat Shah, A. Rashid, MKL Bhatti, "Direct Quadrate (D-Q) Modeling of 3-Phase Induction Motor Using MatLab / Simulink" Canadian Journal on Electrical and Electronics Engineering Vol. 3, No. 5, May 2012.

[25] Nasir Uddin, Muhammad Hafeez, "FLC-Based DTC Scheme to Improve the Dynamic Performance of an IM Drive" *IEEE transactions on industry applications*, Vol. 48, No. 2 March/April 2012.

APPENDIX-A

Open loop simulation of IM :

1.5 KW, 400V, 50Hz,3-phase,4 poles,1440 rpm

R_s = 7.83 ohm, R_r = 7.55 ohm, L_s = 0.4751 H, L_l= 0.4751 H

L_m = 0.4535 H,J = 0.06 kg.m^2, B = 0.01 Nmsec

DTC and FOC:

50HP, 460V,60 Hz,3-phase,4 pole

R_s = 0.087 ohm, R_r= 0.228 ohm, L_s= 0.0355H,

L_r = 0.0355H, L_m = 0.0347H, J = 1.662 kg.m^2,B = 0.1Nmsec

APPENDIX-B

Simulation model of Indirect FOC based on SVPWM

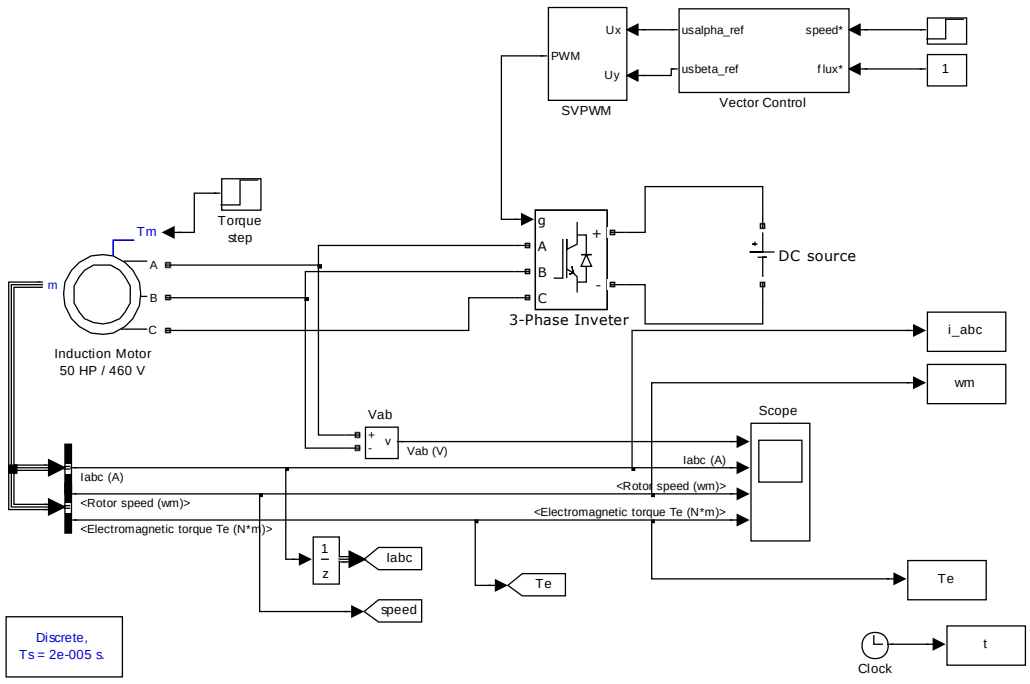

b. DTC controller

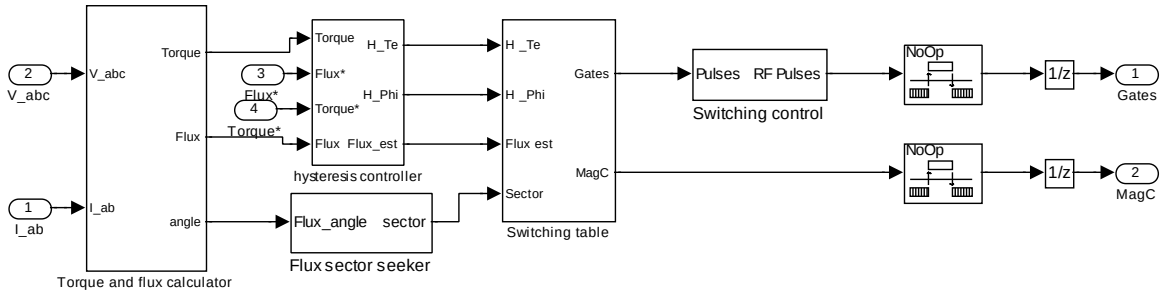

Matlab coding:

a. For sector selection

```
functionSn = S(Ux,Uy)
theta=atan2(Uy,Ux)*180/pi;
if theta>=0&&theta<60
Sn=1;
elseif theta>=60&&theta<120
Sn=2;
elseif theta>=120&&theta<180
Sn=3;
elseif theta>=-180&&theta<-120
Sn=4;
elseif theta>=-120&&theta<-60
Sn=5;
elseSn=6;
end
```

b. For duty cycle calculation

```
function [duty1,duty2,duty0] = fcn(alpha,z0,z1,z2,m)
z3=sqrt(z0*z0+z1*z1);
%vref=2*z2/3
duty1=(2/sqrt(3))*sin(pi/3-alpha)*(m);
duty2=(2/sqrt(3))*sin(alpha)*(m);
duty0=1-(duty1+duty2);
```